Radiochemical studies of nuclear fission

David James Silvester

"RADIOCHEMICAL STUDIES OF NUCLEAR FISSION"

THESIS

presented in candidature

for the degree of

DOCTOR OF PHILOSOPHY

in the

UNIVERSITY OF DURHAM

by

DAVID JAMES SILVESTER, B.Sc. (Dunelm)

The work described in this Thesis was carried out in the Londonderry Laboratory for Radiochemistry, University of Durham, between September 1954, and September 1957, under the supervision of Mr. G.R. Martin, B.Sc., A.R.C.S., F.R.I.C., Reader in Radiochemistry.

ABSTRACT

The relative yields of 19 nuclides* have been measured in the 14-MeV neutron-induced fission of natural uranium, and have been shown to fall on the familiar type of double-peaked mass-yield curve. The measurements on the two xenon isotopes (^{133}Xe and ^{135}Xe) indicate the presence of fine structure in the region of the heavy peak.

The mean peak-to-trough ratio is 9.1, which is of the order expected for fission at this energy, and the best fit for the mirror-points is obtained when ν , the number of prompt neutrons emitted per fission, is taken to be 4.

The condition that the sum of the yields of all the fission-products must be 200% enables values for the absolute yields to be determined: the value so obtained for ^{99}Mo is (6.31 $\pm$ 0.23)%.

A Cockcroft-Walton accelerator was used to produce the 14-MeV neutrons by the D+T reaction. At this neutron energy the cross-sections for ^{235}U and ^{238}U are of the same order of magnitude, so the results are essentially those for the fission of ^{238}U.

---

* (^{83}Br, ^{84}Br, ^{93}Y, ^{97}Zr, ^{99}Mo, ^{105}Ru, ^{109}Pd, ^{111}Pd, ^{111}Ag, ^{112}Pd, ^{113}Ag, ^{115}Ag, ^{129}Sb, ^{131}I, ^{133}Xe, ^{135}Xe, ^{139}Ba, ^{140}Ba, ^{143}Ce).

CONTENTS

CHAPTER 1

INTRODUCTION

Part 1 General

Although many aspects of nuclear fission have been studied since its discovery[1] nearly twenty years ago, a completely satisfactory theoretical understanding of this essentially physical phenomenon is still lacking. At the present time, therefore, it would seem sensible to accumulate as much empirical information about the fission process as possible, in order to facilitate the eventual development of a comprehensive theoretical treatment.

A considerable bulk of such empirical information has, in fact, already accumulated, from a variety of sources. Some has come from the use of purely physical techniques, such as in the measurement of fission-fragment recoil energies with ionisation-chambers or photographic plates; some has come from mass-spectroscopy; but much of it has come from measurements of the yields of the various fission products, using radiochemical techniques of the type to be described in this thesis.

In undergoing fission, a heavy nucleus breaks up into two principal fragments each of roughly comparable mass. Although a number of neutrons may also be released at the instant of fission, the main fragments generally retain

approximately the same neutron-proton ratio as the fissioning nucleus, and since this ratio is normally too high for stability, each decays to a stable isobar by the emission of successive β^- particles, which are frequently accompanied by γ-radiation. "Chains" of isobaric fission-products are thus observed, in some cases with as many as six β-active members. A well-established example of such a chain is that of mass-number 140:-

$$16s\ Xe \xrightarrow{\beta^-} 66s\ Cs \xrightarrow{\beta^-} 12.8d\ Ba \xrightarrow{\beta^-} 40.2h\ La \xrightarrow{\beta^-} \text{stable Ce}$$

A wide range of such β-active fission-products is known, indicating that a variety of modes of fission can occur.

The independent fission-yield of a nuclide is the fraction, or percentage, of the total number of fissions in which that nuclide is formed as an initial fragment. Because of the rapid decay of many of these fragments, independent yields are often difficult to measure experimentally. Moreover, the independent yields of the later members of a mass-chain are generally very small, and do not contribute significantly to the total yield of that mass-number. Frequently, therefore, the total yield of the nuclei of a given mass-number can, with very little error, be identified with the yield of one of the later members of the chain, measured after sufficient time has elapsed for the complete decay of its β-active precursors.

If the absolute fission-yield of one nuclide can be established, others may be found by measuring relative yields. In principle, a direct determination of the absolute yield of a particular nuclide could be made if one knew precisely: (i) the total number of fission events which had occurred in the fissioning material, and (ii) the total number of nuclei of that species which had resulted from the measured number of fissions.

The second of these requirements is not difficult to achieve. If the nuclei are stable, or sufficiently long-lived, they may in many cases be estimated mass-spectrometrically, using an isotopic dilution technique,[2] Thode et al.,[3] in particular, have measured several of the ^{235}U thermal neutron fission-yields in this way, with results which are recokoned to be reliable to within 5%.[4]

Many more results, however, have been obtained from radiometric measurements; the nuclei of one or more of the active members of a mass-chain being counted, by making use of their radioactive properties. Because of the difficulties associated with measuring absolute disintegration rates, the results obtained from such measurements are seldom considered reliable to better than 10%.[4] Recently, however, Baerg and Bartholomew,[5] using 4π counting techniques, have achieved a precision of better than 1.3% in measuring certain relative yields.

The measurement of fission events, on the other hand, presents considerable difficulties, and no great precision can be claimed for the methods available.

One possibility is to count the fission-fragment recoils in a small sample of the material, irradiated simultaneously with the bulk, and subjected to the same flux.[6] Alternatively, in the case of slow-neutron irradiations, the same result may be achieved by counting α-particles, from the $^{10}B(n,\alpha)$ reaction, in a BF_3 flux-monitor.[7] Conversion to fissions, however, requires knowledge of the ratio of ^{10}B-absorption cross-section to the appropriate fission cross-section, and such ratios are still not precisely known.

An alternative, if indirect, method for determining absolute fission-yields is available, however.

If the yields are expressed as percentages, then, since each fission results in the formation of two main fragments, the sum of all the yields should be 200%.

It is customary to plot curves ("mass-yield" curves) to show the mass distribution of the fission fragments, and such curves are essentially symmetrical about a mid-point representing fission into two equal masses, after allowance has been made for the emission of a number of neutrons at the instant of fission.

It will be apparent, therefore, that if sufficient data are available to enable an accurate curve to be drawn showing the relative yields of the various mass-numbers, then the

curve may be normalised to obtain the absolute yields by imposing the condition that the sum of the yields (the area under the curve) must be 200%. This method has been adopted with the results reported in this thesis.

It should be mentioned that α-particles, and some other light nuclei, have been reported by some authors to occur amongst the fission-products with a frequency corresponding to as much as 1% of binary fissions. Recently, however, de Laboulaye et al.[8] have suggested that the light fragments are probably knock-on atoms, and they report that such fragments occur only in 1 ± 3 of 1000 binary fissions.

True ternary fission, into three fragments of comparable mass, has been theoretically predicted, but experimental investigations have only succeeded in showing that such events must be exceedingly rare relative to binary fissions - certainly not frequent enough to affect the normalisation of a mass-yield curve. Work which has been done in this field has been reviewed by Whitehouse.[9]

Fission yields are a function of the nature and energy of the fissioning nucleus. Low energy fission - typified by the thermal neutron fission of ^{235}U - is predominently asymmetric. The mass-yield curve, in such a case, therefore consists of two peaks, with a deep trough between them. For ^{235}U, the peak yields are around mass 95 and 140, the trough is round mass 118, and the peak-to-trough ratio is about 600-to-1.[10]

Further, in low energy fission marked irregularities have been found in certain regions of the mass-yield curve. This "fine-structure" has been attributed to the preferential formation, either at the instant of fission or after the emission of a "delayed" neutron, of nuclei with closed shells of neutrons or protons.

When the energy of the fissioning nucleus increases, as, for example, in the fission of ^{235}U by 14-MeV neutrons,[10] the occurrence of both symmetrical, and very highly asymmetrical, modes of fission increases, at the expense of the moderately asymmetrical modes. The shape of the mass-yield curve alters in consequence: thetrough fills up and the wings splay out slightly, whilst the two peaks must correspondingly become lower. In addition, fine-structure seems to be less marked, suggesting that closed shells of nucleons have smaller influence on the fission process, though this might in some cases be due to less extensive measurements having been made of high energy fission-yields.

Finally, at very high energies symmetrical fission predominates, and the mass-yield curve then consists of a single peak - the height and width of which depends on the energy of the fissioning nucleus - with no fine structure. One of the earliest examples to be observed of this type of fission was that of ^{209}Bi bombarded with 190-MeV deuterons.[11]

The fission of natural uranium (^{238}U 99.28%; ^{235}U 0.715%

^{234}U 0.0058%) has already been the subject of several investigations. Detailed mass-yield curves can now be drawn for its fission by thermal neutrons[10] (essentially ^{235}U fission) and by fission-spectrum (2-3 MeV) neutrons[10] (essentially ^{238}U fission). Yields have also been measured for its spontaneous fission,[12-14] and for fission induced by 16-MeV γ-radiation,[15] by high energy protons, deuterons, helium ions,[16-20] and heavy ions such as ^{12}C, ^{13}C, and ^{14}N.[21-23]

It was to see whether the mass-yield curve for fission of natural uranium by 14-MeV neutrons conformed with the general pattern of such curves that the present work was undertaken. For neutrons of this energy, the fission cross-sections of ^{235}U and ^{238}U are likely to be of the same order of magnitude (for 3 -MeV neutrons, $\sigma_f{}^{238}U \simeq 2^{24}$). This means that the contribution from ^{235}U fission can be ignored, and the results considered to be effectively those for ^{238}U fission.

Until the experimental work to be described here was completed, the only published work on fission by 14-MeV neutrons concerned ^{235}U.[25-27] Recently, however, Cuninghame[28] has published some results for natural uranium. Most of the points he obtained lie on the wings of the mass-yield curve, and he was therefore unable to show the presence of any fine structure; otherwise his results seem to be in quite close agreement with those reported here. A discussion of these results will be found in chapter 7.

Useful reviews of the many publications in the field of nuclear fission have been made by Whitehouse,[9] and more recently by Glendenin and Steinberg[4,28] (low energy fission), and Spence and Ford[30] (high energy fission), whilst an invaluable introduction to the radiochemical approach to the subject may be found in the collection of papers edited by Coryell and Sugarman.[31]

Part 2 The Present Work

The experimental procedures adopted in the work associated with this thesis are fully described in the four chapters which follow, but it may be useful to summarise them at this point.

Natural uranium, in the form of uranyl nitrate, was irradiated with 14-MeV neutrons produced by the D + T reaction, making use for this purpose of the Cockcroft-Walton accelerator built at this laboratory by E.B.M. Martin and G.R. Martin. A brief description of the neutron-generator and its associated monitoring equipment will be found in Chapter 2, which deals with irradiation procedures.

After irradiation, the appropriate carriers were added to the uranyl nitrate and certain of the fission-products were isolated by chemical techniques. In deciding which of the many known fission-products could usefully be separated from the irradiated uranium, several factors had to be taken into account. Nuclides with complex, or incompletely known, decay schemes were not suitable for radiometric determination, neither were those with half-lives shorter than about 20 minutes (because of the time involved in their separation) or longer than a few days (because of their low intensity).

Chemical separation procedures were worked out, or adapted from unpublished information, for eleven elements (Br, Y, Zr, Mo, Ru, Pd, Ag, Sb, I, Ba, Ce) but because of the

rapid decay of many of the species involved it was seldom possible for one person to make measurements on more than a few elements at one time. In order to make the best use of the irradiated material, therefore, the Ru, Pd, Ag, Ce, and several of the Mo, separations were carried out by Mr. R.H. James (Research Assistant at this laboratory), with whom the sometimes arduous task of "counting", i.e. measuring the activities of, the separated samples was also shared.

To inter-relate the results of the various runs, barium was separated in each case, and the yields of all the nuclides were determined relative to that of ^{139}Ba.

The chemical separations for which the author was responsible, together with the techniques used in mounting and counting the active samples, are fully described in Chapter 3. For the sake of completeness, the procedures used by Mr. James in the Ru, Pd, Ag, and Ce separations are also summarisedthere.

Some further experimental work was carried out, to determine the effect on the results of fission induced by the D + D neutrons produced by the neutron generator. This is reported in Chapter 4, together with the work on the measurement of sellotape absorption factors, and the growth curve for ^{140}Ba-^{140}La.

The results obtained for the elements mentioned above were sufficient to enable a smooth mass-yield curve of the expected double-humped shape to be plotted. In order to

fill in a gap in the heavy peak, however, and to look for possible fine-structure in this region, the yields of two xenon isotopes (^{133}Xe and ^{135}Xe) were also investigated. This required a quite different kind of experimental procedure from that used for the other elements.

A special apparatus was designed and built to enable xenon to be separated from an irradiated solution of uranyl nitrate, and purified from other fission-products, and a suitable method of measuring the activity of the gas so obtained was also devised. The experimental work connected with the measurements on the xenon nuclides is described in Chapter 5.

The results obtained, for all the fission-yields which have been investigated, are reported in Chapter 6, where also the methods of calculation are discussed. A summary, and discussion, of these results is given in Chapter 7.

CHAPTER 2

THE FAST-NEUTRON IRRADIATIONS

Part 1 The Neutron Source

The D + T reaction may be represented by the equation:

$$^{2}H\ (D) + {}^{3}H\ (T) \longrightarrow {}^{4}He + {}^{1}n + 17.6\ MeV$$

As well as being highly exoergic, this reaction has a very high, broad resonance for 100-keV deuterons striking a thin tritium target. This means that only comparatively low-voltage accelerating equipment is required in order to make use of the reaction as a source of copious quantities of high-energy neutrons. Further, due to the absence of excited states in ^{4}He, such neutrons have the merit of being essentially mono-ergic, at about 14-MeV.[32]

At this laboratory, a beam of deuterons of suitable energy is produced by the Cockcroft-Walton type of accelerator which has been described elsewhere by E.B.M. Martin.[33] In this machine, the deuteron beam impinges on a target consisting of tritium absorbed in a thin film of zirconium metal. The zirconium film is supported on a copper or silver foil which is, in turn, soldered to the copper target-block of the accelerator. During an irradiation, about 40 watts are dissipated in the target-block: this is therefore water-cooled to reduce the loss of tritium due to the heating

of the target.

Using this apparatus, the neutron yield has been found to improve as the deuteron energy is increased up to about 200-keV, but above that energy the yield begins to drop again. Beam currents of up to 500 μa have been obtained with this machine in favourable conditions, but throughout most of the 20-odd irradiations reported here the beam current was in the region of 200 μa.

For 200-keV deuterons and a thick zirconium-tritium target, the yield is reported[32] to be about 10^8 neutrons per sec. per microampere, and our own very rough estimates of the neutron yield, made by measuring the activity induced in a copper disc, are in agreement with this figure, about 10^9 or 10^{10} neutrons per sec. being obtained from a fresh tritium target.

The neutron energy varies to some extent with the angle of emission. Over the solid angle within which the uranium samples were irradiated, however, this variation amounts to less than ± 3% of a mean energy of about 14.4-MeV, which is negligible in its effect on the measured fission-yields.

The tritium targets are supplied by A.E.R.E. Harwell, and as supplied, each target disc contains about a curie (about 0.2 ml STP) of tritium (12.3y ^3H). For reasons of economy each disc is cut into four segments which are bombarded separately. A method of preparing such tritium

targets has been described by Graves et al.[34]

It has always been observed that the neutron yield from a target segment drops quite considerably during the course of deuteron bombardment, frequently, after about 4 hours, to as little as 20% of the initial yield. Probably two factors are chiefly responsible for this. Firstly, tritium may be lost from the target because of the local heating effect of the deuteron beam, particularly if the target has been poorly soldered to the cooled target-block. Secondly, because the target-block is at a lower temperature than its surroundings, a considerable deposit of carbon (decomposed pump oil) builds up on the target surface, which reduces the penetration of the deuteron beam to the tritium beneath. An attempt was made to reduce this carbon deposition by passing the deuteron beam through a liquid-air cooled tube just above the target, but this was found to have little effect.

Deuterium, too, inevitably builds up on the target in the course of bombardment, and this leads to the production of lower energy neutrons, of about 2.5 MeV, from the D + D reaction. The effect of these neutrons has been investigated, with the results reported in Chapter 4.

Part 2 The Neutron Monitor

As has been stated above, the neutron yield from a given tritium target generally dropped quite markedly in the course of deuteron bombardment, and for this reason fast-neutron irradiations of more than 4 hours duration were not attempted. Superimposed on this general effect, however, there were more random fluctuations in the neutron flux which were due to variations in the intensity and positioning of the deuteron beam.

The effect of this variable neutron flux was, of course, different for fission-products of different half-lives. To enable this to be taken into account in calculating the fission-yields, therefore, the neutron flux was monitored throughout the irradiations.

In the first two runs, this was achieved by counting disintegrations and recoils in a BF_3-filled proportional counter, which was mounted in a large block of paraffin-wax and placed in a fixed position relative to the neutron source. This counter was not satisfactory, since it did not discriminate between fast and slow neutrons, and it was therefore replaced by one which did.

This took the form of a scintillation counter, having as its phosphor an organic plastic crystal ("Pamelon") in which proton recoils were counted. The discriminator bias voltage

was set above the threshold for counting the D + D neutrons (2-3 MeV), so that only the higher energy D + T neutrons were recorded.

During the irradiations, neutron-monitor readings were recorded at regular intervals. In irradiations of 60 minutes or less, these intervals were generally of 5 minutes; in longer irradiations they were 10 minutes. The method of calculating the "irradiation factor" for each fission-product, making use of these readings, is given at the beginning of Chapter 6.

Part 3 Target Material

The stock of natural uranium used throughout this work took the form of Analytical Grade uranyl nitrate hexahydrate, $UO_2(NO_3)_2 6H_2O$, (U.N.H.). In the first 20 runs, this was irradiated in the crystalline form, and it was not found necessary to remove from it any of the daughter activities (UX_1, UZ, UY, etc.) which would have grown into it since it was last purified by the manufacturer.

Depending upon the number of fission-products which were to be separated from the irradiated material, between 10 and 60 g of U.N.H. were taken for each run. To speed solution afterwards, this was ground to a fine powder, and then simply wrapped into a filter-paper packet and strapped beneath the target-block of the neutron generator for irradiation.

In the work on the Xenon isotopes, solutions of uranyl nitrate were irradiated in a specially designed vessel. The presence of a significant amount of radium was detected in these solutions (see Chapter 5), but this was easily removed by the following procedure:

To the U.N.H. solution about 20 mg of barium carrier were added. The addition of 5 mls 2M H_2SO_4 precipitated $BaSO_4$, and this carried down with it the trace quantities of radium which were present in the solution. After allowing it to stand until the precipitate had begun to settle, the solution was filtered through a Whatman No 3 filter-paper. The

$BaSO_4$ precipitation was repeated by the addition of a further 20 mg of barium carrier to the filtrate, and, after a second filtration, the solution was evaporated down to its original volume once more.

Recovery of Uranium from Residues

From time to time the uranium was recovered from the collected residues of each run, for use in further irradiations. The purification cycle adopted was as follows:-

1. The acid residues were neutralised with $(NH_4)_2CO_3$, and sufficient excess was added to bring all the uranium into solution as $(NH_4)_4\ [UO_2(CO_3)_3]$.

2. This solution was filtered from insoluble carbonates (notably Ba, Sr, and Ce) and other insoluble material, and the filtrate was carefully acidified with HNO_3.

3. After boiling off all the CO_2 from the solution, concentration of the residues was effected by precipitation of the uranium as $(NH_4)_2U_2O_7$ with NH_4OH. This precipitate was filtered and washed.

4. The precipitate was dissolved in the minimum quantity of HNO_3 and extracted into ether, using a continuous liquid-liquid extraction apparatus.

5. The uranium was back-extracted into water containing a little HNO_3, and the solution evaporated to a small bulk before being set aside to allow the U.N.H. to crystallise out.

CHAPTER 3

THE PREPARATION OF SOURCES FOR THE 2π-COUNTER

Part 1 General Procedure

After irradiation, the packet of U.N.H. was allowed to remain beneath the target-block of the neutron generator for two or three minutes to permit the decay of the very short-lived fission-products, and to reduce the γ-activity somewhat, before it was removed to the laboratory where the various chemical separations and radiometric determinations were carried out. The time of the end of each irradiation was very carefully noted, and was taken as the reference time for comparing the activities of the isolated fission-products.

The U.N.H. was dissolved in 0.1M HNO_3, roughly 2.5 mls of solvent being used for each g. of irradiated U.N.H. From this "stock-solution" aliquots were removed by means of a manually operated pipette for each of the chemical procedures; in only one case (Ag/Ba) were two elements isolated from a single aliquot.

To each of these aliquots, known amounts of the appropriate inactive carriers were added, and the chemical separation procedures described later in this chapter were carried out. The essential requirement, in all these chemical procedures, was a sufficiently rapid means of preparing a sample of each fission-element, free from contaminating activities, in a

form suitable for counting. It should be stressed that, provided the sample was also suitable for the gravimetric determination of the recovered carrier, a rigorously quantitative analytical procedure was not necessary.

The chemical procedures were so arranged that the final precipitate, consisting of the required fission-product with its inactive carrier, could be separated by filtration through a specially made "filter-stick" (Fig. I). By this means, the precipitate was spread uniformly over a circle, 1.6 cm in diameter, on a small Whatman No. 3 filter-paper disc, which could be placed in an aluminium tray for counting.

Chemical yields were determined by direct weighing, and so as to minimise the errors involved in these measurements, the same standard routine was followed in the preparation of all the solid sources. Each filter-paper disc was prepared for use by mounting it in the filter-stick and washing it successively with 3 x 5 mls of water, ethanol, and dry ether. It was then placed in a vacuum desiccator which was evacuated for 2 minutes, opened to the atmosphere, and then evacuated for a further 5 minutes. The disc was then quickly transferred to a small weighing-bottle, which had a tightly-fitting ground-glass lid, in which there was no risk of the disc absorbing moisture from the atmosphere, and hence gaining weight, during weighing. (One such disc, in this vessel, was found to increase in weight by less than 0.05 mg in 0.5 hour: weighing usually took less than 2

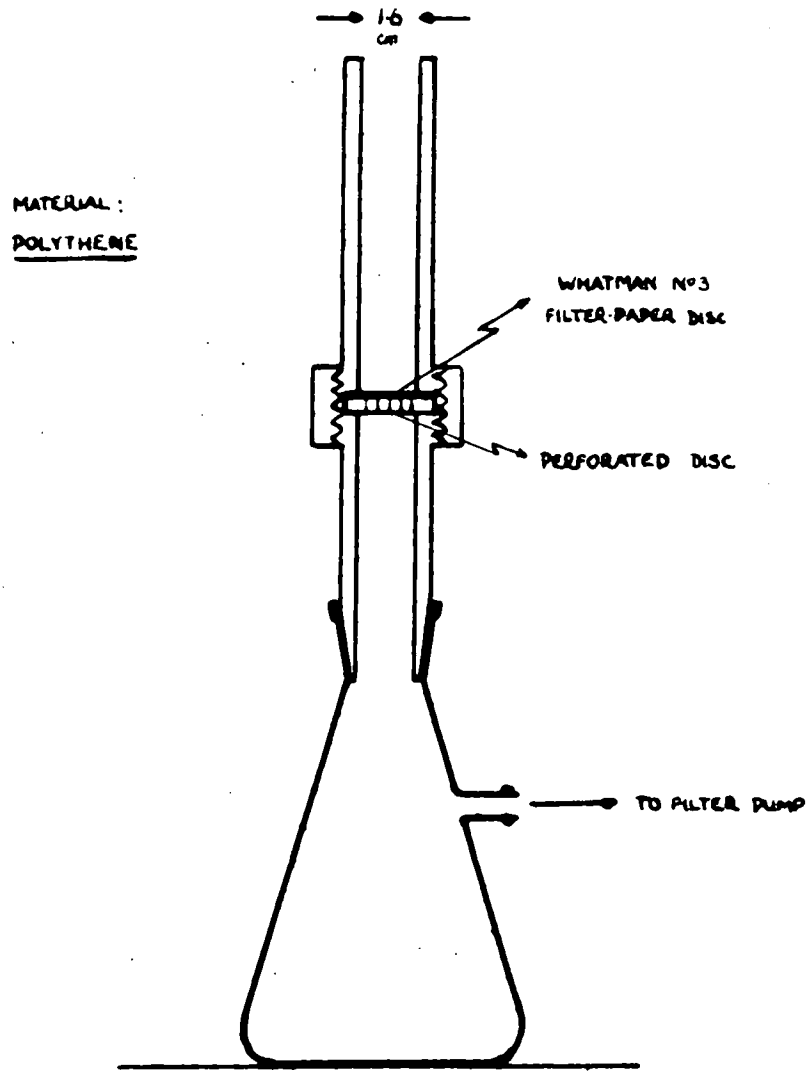

FIG. I FILTER-STICK.

minutes). A Stanton semi-micro balance (Model MC1A) was used, and the discs were weighed to the nearest 0.01 mg.

Precisely the same procedure was adopted in washing, drying, and weighing the discs after the active precipitates had been filtered on to them.

The weight of each sample was generally about 10 to 20 mg. This weight was certainly accurately known to within ± 0.1 mg, so the chemical yield factors, determined in this way, were accurate to within about ± 1%.

Part 2 The Counting Equipment

All the solid sources, prepared by the method just described, were counted in the gas-flow 2π β-proportional counter of A.E.R.E., Harwell, manufacture (Type 1222A) shown in Fig. II. The gas used was methane, obtained from the Point of Ayr Colliery pit-drainage scheme. After purification from O_2 and H_2O, by passage through tubes containing heated platinum gauze and "Anhydrone", the gas flowed through the counter at little more than atmospheric pressure.

It was early found that the counting rate of a standard source depended to some extent on the gas flow-rate. A simple flow-meter was therefore attached to the outflow side of the counter, and the gas flow was regulated, during counting, to 0.6 ml/sec.

The electronic apparatus, and the gas-flow system, associated with the counter, are shown diagrammatically in Fig. III. Using an anode loop of 1 thou. constantan wire (see Fig. II) the threshold voltage for counting was at about 2.4 kV. Above this voltage, the counter normally gave a plateau more than 400 V long. The scaler paralysis time was set at 5 μsec, which made corrections for "dead-time" insignificant, even for counting rates as high as 10^5 c.p.m.

Except for a small gap at one end, through which access was obtained for changing sources, the counter was entirely

FIG. II

2π-β-PROPORTIONAL COUNTER

A.E.R.E. TYPE 1222A

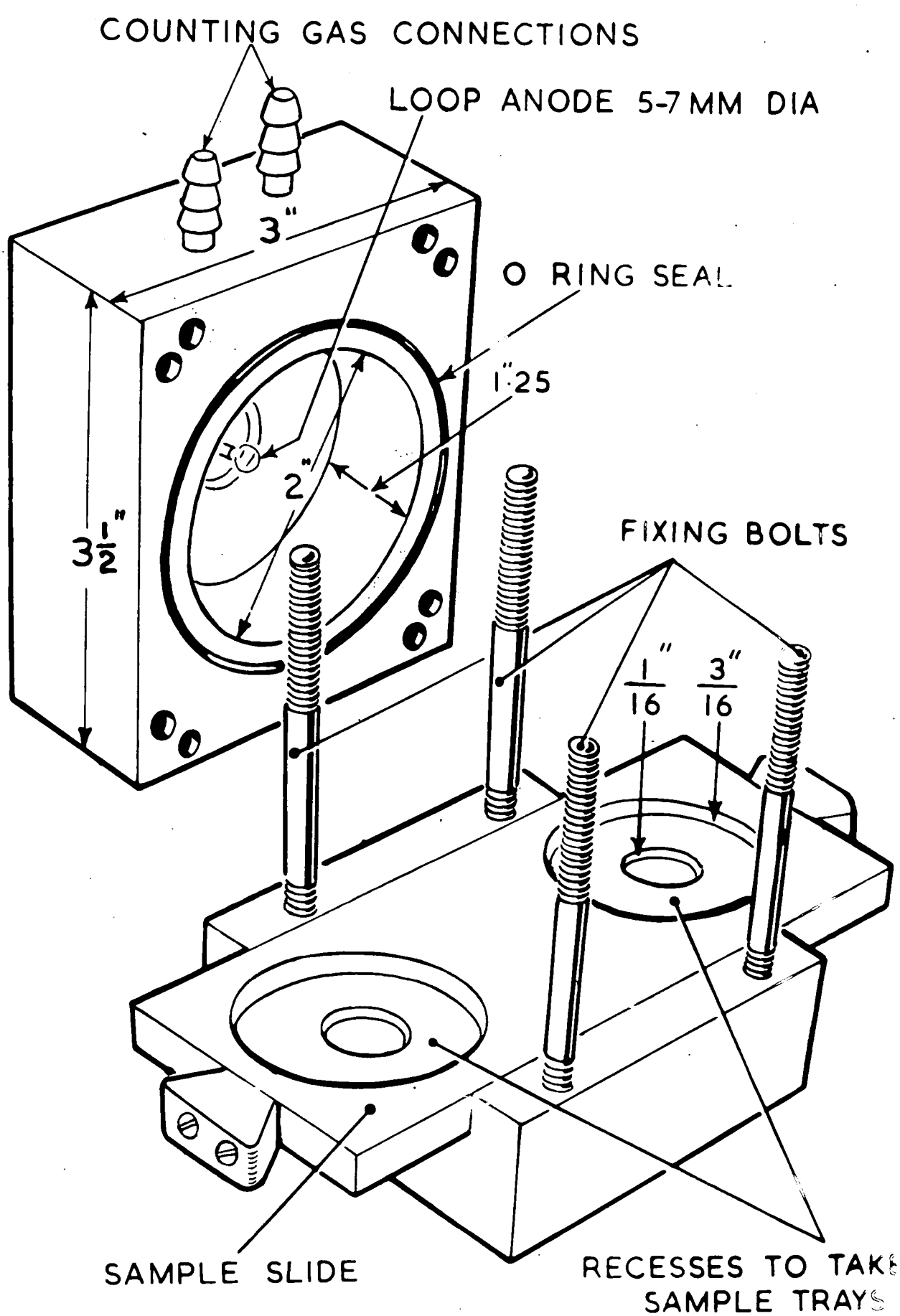
COUNTING GAS CONNECTIONS
LOOP ANODE 5-7 MM DIA
3"
O RING SEAL
1·25
2"
3 1/2"
FIXING BOLTS
1/16"
3/16"
SAMPLE SLIDE
RECESSES TO TAKE
SAMPLE TRAYS

surrounded by 1.25" lead shielding. The background count, inside this shielding, was about 40 c.p.m.

As can be seen from Fig. II, the sources, on their aluminium trays, were placed inside the sensitive volume of the counter, so this had to be momentarily opened to the atmosphere each time one source was replaced by another. It was therefore necessary to flush the counter thoroughly before each source was counted. To do this, the methane flow rate was increased to about 3 mls/sec for a minute and then reduced to its normal rate for a further 4 minutes before counting started. If the flow rate was not increased for a while, the counter was found to take more than 10 minutes to settle down to a steady counting rate.

A frequent source of trouble, when using this counter, was the O-ring seal between the main body of the counter and the sample slide. This developed the habit of popping out of place as the slide was moved from one position to another in the course of changing sources, often damaging the sources - and getting contaminated with active material - in doing so. To prevent this happening at times when several sources had to be counted in rapid succession, the sources were protected by covering them with a layer of Sellotape, though this meant that a "Sellotape absorption factor" had to be determined for each nuclide measured in this way. (See Chapter 4, Part 2).

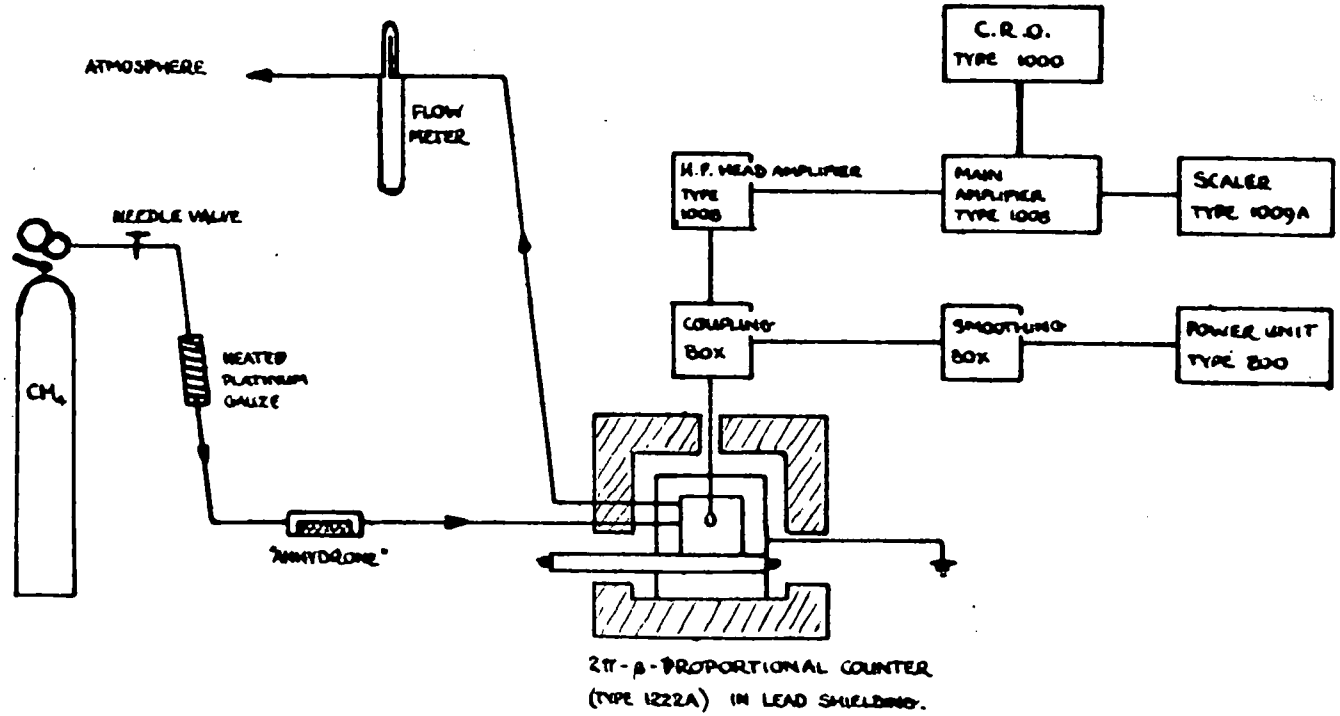

FIG. III : GAS-FLOW SYSTEM, AND ELECTRONIC EQUIPMENT, ASSOCIATED WITH THE 2π - COUNTER.

The decay of each source was followed for at least six half-lives or until its activity was too low for reliable determination. The decay-curves so obtained were then resolved, when necessary, and extrapolated back to determine the activity due to each nuclide at the end of the irradiation. This extrapolated, or "observed", activity was then divided by a number of correction factors (for chemical yield, sellotape absorption, self-absorption, and, where applicable, for daughter activity) in order to obtain the "corrected" activity which was required for the determination of the relative yields of the different nuclides. (See Chapter 6).

The counting-rate given by a standard source in the 2π-β-proportional counter was some five times greater than that obtained with the same source under an end-window Geiger-Mueller counter, using "top-shelf" geometry. The background, on the other hand, was little more than double that of most counter tubes. Thus, in spite of the drawbacks associated with its use, there is no doubt that the 2π-counter was the best available at the time for counting the low intensity samples obtained of the low-yield, or long-lived, fission-products.

Part 3 Chemical Separation Procedures

(a) BARIUM

The yields of ^{139}Ba and ^{140}Ba were determined: the decay chains for these masses are as follows[35]:-

139: 2.7sI → 41s Xe → 9.5m Cs → 85m Ba → st La

140: 16s Xe → 66s Cs → 12.8d Ba → 40.2h La → st Ce

The method used in the isolation of barium from the fission-product mixtures was the classical one of repeated precipitation as $BaCl_2.H_2O$ using a mixture of HCl and ether. A suitable $Ba(NO_3)_2$ carrier solution was prepared, and standardized as $BaCl_2.H_2O$, by the method described by Glendenin.[36]

In many runs, silver and barium were both isolated from a single aliquot of the solution of irradiated U.N.H. (afterwards referred to as the "stock-solution"). Not less than 90 minutes were always allowed for the 9.5m ^{139}Cs to decay before beginning the barium separation.

Procedure:

Step 1. 1 ml each of the standardized barium and silver carrier solutions, containing approximately 10 mg Ba and Ag, were added to a 20 ml aliquot of the stock-solution, and the silver separated as AgCl (by R.H.J.) by the addition of 2 mls 5M HCl. The supernate (or, for samples from which silver was not to be isolated, the original solution with no silver carrier present) was then evaporated down to about

3 mls in a small beaker on a hot-plate.

Step 2. 20 mls of ether/HCl mixture (1 part ether to 5 parts conc. HCl) were added, and the solution transferred to a 50 ml centrifuge tube. The beaker was rinsed with a further 20 mls of ether/HCl, and the rinsings added to the solution in the centrifuge tube, which was then clamped under the cold tap. The solution was stirred vigorously, until precipitation of the $BaCl_2.H_2O$ was complete. After centrifugation, the supernate was removed from the precipitate by means of the simple device shown in Fig. IV. Attempting to decant the solution in the normal way invariably disturbed the precipitate, there being not much difference in the densities of the two phases.

Step 3. The $BaCl_2.H_2O$ was dissolved in 2 mls H_2O, and was then reprecipitated by addition of 30 mls of ether/HCl, cooling and stirring the solution as before. The precipitate was separated as in the previous step.

Step 4. Step 3 was repeated.

Step 5. The $BaCl_2.H_2O$ was washed twice by centrifugation with 5 mls of ethanol, containing 4% HCl to reduce its solubility, then slurried with 5 mls of the same solution and transferred, by filtration through the filter-stick, to a weighed filter-paper disc. After washing with 3 x 5 mls of dry ether, the disc with the precipitate of active $BaCl_2.H_2O$ was dried and weighed by the method already described, and

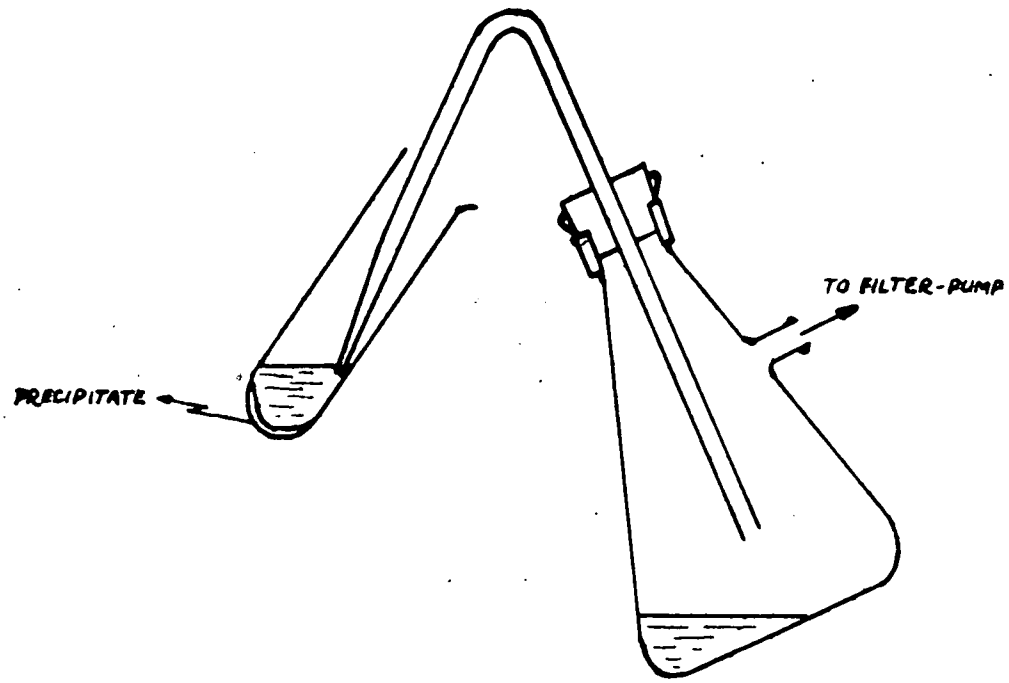

FIG. IV: DECANTING DEVICE

was then ready for counting.

This precedure took only about 30 minutes to complete, and was found to give radiochemically pure barium samples, without the addition of a $Fe(OH)_3$ scavenging precipitation. The results are reported in Chapter 6. Those for ^{139}Ba, which was adopted as a reference nuclide, are shown in Table III; those for ^{140}Ba are shown in Table XVII, whilst a discussion of the growth of ^{140}La activity in the barium samples is given in Part 3 of Chapter 4.

(b) BROMINE AND IODINE

The yields of ^{83}Br, ^{84}Br and ^{131}I were determined: the decay chains for these masses being[35]:-

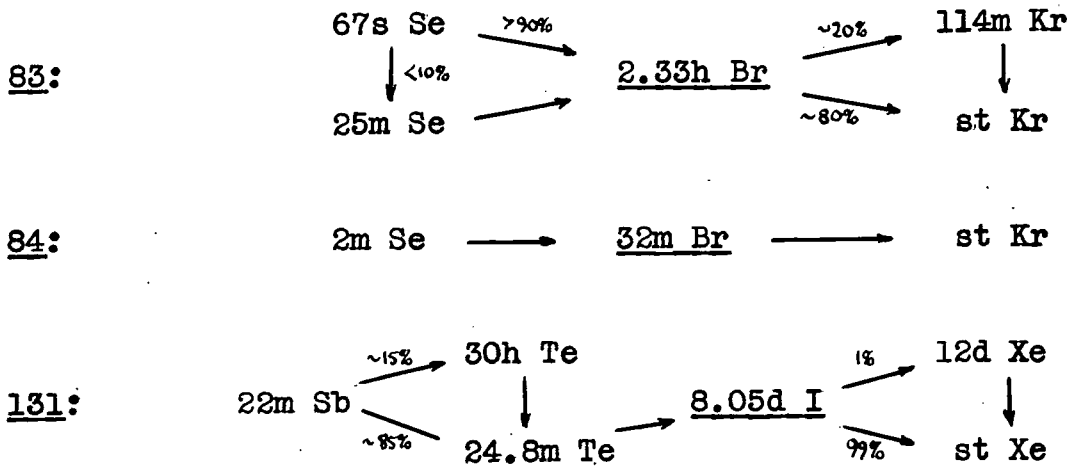

Although the bromine and iodine separations are similar in the initial stages, and are therefore conveniently described together, the two elements were never, in fact, both isolated from the same aliquot of stock-solution for yield measurement

purposes. This was because it was necessary to delay the iodine separation for about 48 hours to allow for the decay of its precursors, and of short-lived iodine nuclides, whilst the 32 m half-life of ^{84}Br required that the bromine separation should be performed as quickly as possible after the end of the irradiation. (30 minutes delay was allowed for the decay of ^{83}Se).

The separation methods adopted were based on those described by Glendenin et al.[37,38] The procedures begin with oxidation and reduction steps, to ensure complete exchange between the tracer bromine and iodine and their respective carriers. The KBr and KI carrier solutions were prepared and standardized by the method of Glendenin and Metcalf,[38] except the precipitates were dried in a vacuum desiccator instead of an oven.

Procedure:

Step 1. 1 ml each of the standardized bromine and iodine carrier solutions (containing approx. 10 mg of I and Br) were added to a 20 ml aliquot of the stock-solution. The solution was made alkaline, and the uranium complexed, by the addition of a solution of 4 g Na_2CO_3 in 15 mls water, warming the mixture, if necessary, to effect complete solution. 2 mls of 5% NaClO were then added, and the solution was warmed and thoroughly stirred. This oxidised the Br^- to BrO_3^- and the I^- to IO_4^-. After cooling, the solution was transferred to a separatory funnel.

Step 2. The solution was next acidified by the careful addition of 5 mls of conc. HNO_3, drop by drop. After adding 2 mls 6% $NH_2OH.HCl$, which reduces BrO_3^- to Br^- and IO_4^- to I_2, the I_2 was extracted into two 10 ml portions of CCl_4. The organic phase was retained for the iodine separation (Step 8 onwards), and the bromine separation was continued as follows:

Bromine separation:

Step 3. To the aqueous layer from step 2, 1 ml of conc. HNO_3 was added, followed by a solution of $KMnO_4$, drop by drop until the solution retained a purple colour. The Br^- was thereby oxidised to Br_2, which was then extracted into two 10 ml portions of CCl_4. The aqueous layer was discarded.

Step 4. The CCl_4 layer was shaken up with 10 mls of water containing a few drops of 6% $NH_2OH.HCl$, which reduces Br_2 to Br^-, until the two phases were colourless. The CCl_4 was then discarded. (N.B. Any I_2 present at this stage remained in the organic phase - giving it a faint purple colour).

Step 5. After adding 2 mls of 5M HNO_3 and sufficient $KMnO_4$ to colour the solution permanently, the Br_2 was once more extracted into CCl_4 and the aqueous layer discarded.

Step 6. The CCl_4 layer was shaken up with 10 mls of water

containing a few drops of 1M $NaHSO_3$ until both phases were colourless (Br_2 reduced to Br^-). The organic phase was discarded.

Step 7. 2 mls of 5M HNO_3 were added, and the solution raised to about 80°C to expel SO_2 before the bromine was precipitated by the addition of 2 mls of 0.1M $AgNO_3$. After digesting the precipitate for a few moments, it was transferred, through the filter-stick, to a weighed filter-paper disc. The precipitate was washed, dried, and weighed in the usual way.

Iodine separation:

Step 8. The organic layer from step 2 was shaken up with 10 mls of water containing a few drops of 1M $NaHSO_3$, which reduces I_2 to I^-, until both phases were colourless. The CCl_4 was discarded.

Step 9. 2 mls of 5M HNO_3 and a few drops of 1M $NaNO_2$ were added, oxidising I^- to I_2, and the iodine was extracted into CCl_4. The aqueous layer was discarded.

Step 10. The CCl_4 layer was shaken up with 10 mls of water containing a few drops of 1M $NaHSO_3$, until both phases were colourless. The CCl_4 was discarded.

Step 11. 2 mls of 5M HNO_3 were added, and the solution raised to about 80°C to expel SO_2 before the iodine was precipitated by the addition of 2 mls of 0.1M $AgNO_3$. After digesting the precipitate for a few moments, it was transferred,

through the filter-stick, to a weighed filter-paper disc. The precipitate was washed, dried, and weighed in the usual way.

Each of these procedures took about 45 minutes to complete and gave sources which decayed with the expected half-lives. The results are reported in Chapter 6. Those for ^{83}Br are shown in Table IV; those for ^{84}Br in Table V; and those for ^{131}I in Table XVI.

(c) YTTRIUM

The yield of ^{93}Y was determined: the decay chain for this mass-number being[35]:-

93: short ⟶ 7m Sr ⟶ 10.0h Y ⟶ 1.1×10^6 y Zr ⟶ st Nb

An yttrium nitrate carrier solution was prepared and standardized as $Y_2(C_2O_4)_3.7H_2O$ by the method of Ballou.[39]

The method used in the isolation of yttrium from the fission-product mixtures was based on that reported by Ballou.[39] The modifications, which speeded up the separation somewhat, were the use of T.B.P. (tri-n-butyl phosphate), first to extract uranium, and later to extract cerium (IV) from the mixed rare-earths and yttrium.

Procedure:-

Step 1. 1 ml of the standardized yttrium carrier solution (containing approx. 10 mg Y) together with 1 ml each

of cerium (III), lanthanum, and zirconium carriers, and 5 mls of conc. HNO_3, were added to a 20 ml aliquot of the stock-solution in a separatory funnel. At this acidity, practically all the uranium could be extracted into 15 mls of T.B.P., which was then discarded, whilst the trivalent elements remained in the aqueous phase.[40]

Step 2. The aqueous solution from step 1 was evaporated down to about 2 mls, and then made up to 8 mls with 2M HNO_3 and transferred to a polythene centrifuge tube. On the addition of 2 mls conc. HF, yttrium and rare-earth fluorides were precipitated (zirconium and uranium remain in solution at this stage) and were separated by centrifuging, followed by decantation. The precipitate was washed with 10 mls of 1M HF.

Step 3. The precipitate was dissolved in 2 mls water, 2 mls 5% H_3BO_3, and 1 ml conc. HNO_3. 1 ml of zirconium carrier solution was added, followed by 2 mls conc. HF. The precipitated fluorides were once more separated and washed.

Step 4. The precipitate was dissolved in 2 mls water, 2 mls 5% H_3BO_3, and 1 ml conc. HNO_3, and the clear solution transferred to a 50 ml pyrex centrifuge tube. Yttrium and rare-earth hydroxides were then precipitated by the addition of excess conc NH_4OH. Any barium or strontium carried by the rare-earth fluorides was removed by this step.

The precipitate was washed with water.

Step 5. The precipitate was dissolved in 1 ml conc. HNO_3 and the solution diluted to 10 mls. About 1 g $KBrO_3$ was added and the solution was boiled. The solution then became coloured, owing to the oxidation of Ce (III) to Ce (IV). After cooling the solution thoroughly, the $Ce(NO_3)_4$ was extracted into an equal volume of T.B.P.,[41] leaving the aqueous phase colourless once more. The organic layer was separated and discarded.

Step 6. The addition of NH_4OH to the aqueous phase from step 5 precipitated yttrium and lanthanum hydroxides, which were then separated by centrifugation, and thoroughly washed with water. The precipitate was dissolved in 1 ml conc. HNO_3, and the solution diluted to 10 mls. 1 ml of cerium carrier was added and the cerium separation procedure of step 5 was repeated.

Step 7. Yttrium and lanthanum hydroxides were precipitated by the addition of NH_4OH to the aqueous phase from step 6, and the precipitate was centrifuged and washed before being dissolved in 1 ml conc. HCl. The resulting solution was carefully evaporated down to dryness. 3 mls of 50% K_2CO_3 solution were then added, and the solution was warmed until the solid residue had completely dissolved. 20 mls of water were added, and the solution was heated almost to boiling point and stirred continuously. After a few moments, $KLa(CO_3)_2$ was precipitated, and the precipitate took a

crystalline form after maintaining at about 95°C for 5-10 minutes. The solution was centrifuged, and the precipitate discarded.

Step 8. The solution from step 7 was carefully acidified with a little conc. HCl, and most of the liberated CO_2 was boiled off. 1 ml of lanthanum carrier solution was added, and step 7 was repeated.

Step 9. The solution from step 8 was carefully acidified with a little conc. HCl, and most of the liberated CO_2 was boiled off. Yttrium hydroxide was then precipitated by adding NH_4OH. This was separated by centrifugation, and washed with water.

Step 10. The precipitate was dissolved in 1 ml conc. HCl and the solution diluted to 10 mls. The solution was heated almost to boiling, and 10 mls of a saturated solution of oxalic acid were added. After cooling thoroughly in an ice bath, the precipitated $Y_2(C_2O_4)_3.7H_2O$ was separated by filtration onto a weighed filter-paper disc. This was then washed, dried, weighed, and mounted for counting in the usual way.

This procedure generally took about 60 minutes to complete. It was never started until about 2 hours after the irradiation, by which time all the 7m ^{83}Sr precursor of ^{93}Y had decayed. The presence of yttrium isotopes with both longer and shorter half-lives than that of the 10h ^{93}Y was

expected, and observed, in the sources prepared by the above method. It was, however, always possible to resolve the decay-curves in order to determine the activity due to the ^{93}Y.

It will be seen from the table of results (Table VI) that the recovery of the yttrium, using this method, was, in general, somewhat lower than that of the other elements. The reason for this is uncertain, though in the light of a recent publication by Scargill et al.[42] it seems likely that some loss of yttrium may occur at steps 5 and 6, by extraction with cerium into T.B.P.

(d) ZIRCONIUM

The yield of ^{97}Zr was determined: the decay chain for this mass-number being[35]:-

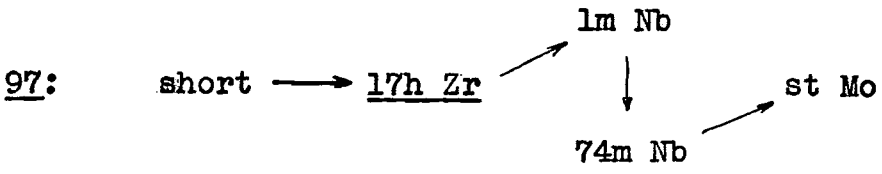

In the first four runs, zirconium was separated from the mixed fission-products by a modification of the method of Hume,[43] the final precipitation being made with mandelic acid, and not with cupferron. The recovery, using this method, was rather low, however.

The extraction method adopted in the later runs was based on a publication by Furman et al.,[44] and had the merit

of being speedier than Hume's, and generally of giving much higher yields.

The zirconium nitrate carrier solution contained about 5 mg Zr/ ml, and a known volume of this was standardized by precipitation with mandelic acid.[45] The zirconium tetra-mandelate ($Zr(CO_2 \cdot CHOH \cdot C_6H_5)_4$) was filtered off, ignited, and the resulting ZrO_2 was weighed.

Procedure 1:-

Step 1. 1 ml each of cerium, lanthanum, yttrium, and the standardized zirconium carriers were added to a 20 ml aliquot of the stock solution in a separatory funnel, and the bulk of the uranium was extracted into two 15 ml portions of ether.

Step 2. The aqueous layer from step 1 was evaporated down to about 5 mls, and transferred to a polythene centrifuge tube. 4 mls of conc. HNO_3 were added, followed by 2 mls of conc. HF. This precipitated yttrium and the rare-earth fluorides, which also carry down the Ba, Sr and UX_1 (Th) activities. After centrifuging, the supernate was transferred to a second polythene tube.

Step 3. 1 ml of lanthanum carrier solution was added, and the precipitated LaF_3 was separated by centrifugation and discarded.

Step 4. The supernate from step 3 was transferred to a third polythene tube, and 1 ml of barium carrier solution (approx. 50 mg Ba) was added. After standing

for 1 minute, the precipitate of $BaZrF_6.H_2O$ was separated by centrifugation, and the supernate discarded.

Step 5. The precipitate from step 4 was dissolved in 5 mls water, 2 mls 5% H_3BO_3, and 1 ml HNO_3. The zirconium was then reprecipitated by addition of 1 ml of barium carrier solution, and 1 ml of conc. HF. After centrifugation, the supernate was discarded.

Step 6. Step 5 was repeated.

Step 7. The $BaZrF_6.H_2O$ was dissolved in 5 mls water, 2 mls 5% H_3BO_3, and 3 mls conc. HCl. A drop of conc. H_2SO_4 was added, and the solution centrifuged. The supernate was decanted from the precipitated $BaSO_4$ into a 50 ml glass centrifuge tube. The solution was made alkaline with 6M NaOH, which precipitated $Zr(OH)_4$. The solution was centrifuged, and the supernate discarded.

Step 8. The precipitate from step 7 was dissolved in 2 mls conc. HCl. The solution was diluted to 10 mls with water, and about 5 drops (5 mg Th) of a thorium nitrate carrier solution were added. 10 mls of a freshly prepared 1M mandelic acid solution (1.5 g in 10 mls water) were added, and the tube was placed in a water-bath until the precipitation of the zirconium tetra-mandelate was complete. The bulky precipitate was then separated and washed by centrifugation, using two 10 ml portions each of water and ethanol, before being slurried with ethanol and transferred

to a weighed filter-paper in the filter-stick. This was then washed with ether, and dried, weighed, and mounted for counting in the usual way.

Procedure 2:-

Step 1. 1 ml of the standardized zirconium carrier solution was added to a 20 ml aliquot of the stock solution, together with 2 mls conc. H_2SO_4. The mixture was transferred to a separatory funnel, 5 mls of chloroform were added, and the two phases stirred mechanically. On the addition of 2 mls of a freshly prepared and filtered 5% cupferron solution, a transient white precipitate of zirconium was observed in the aqueous phase, but this rapidly dissolved in the organic phase. Uranium was not extracted under these conditions.[44] The organic layer was separated, and transferred to a pyrex centrifuge tube.

Step 2. A second 5 ml portion of chloroform was added to the separatory funnel and the mixture was again stirred mechanically before the organic layer was separated, and added to the first sample.

Step 3. The tube containing the organic fractions from steps 1 and 2 was placed in a boiling water-bath, until the chloroform had completely evaporated. It was then removed, 2 mls of conc. H_2SO_4 were added to the residue, and the tube was very cautiously heated over a bunsen flame, adding conc. HNO_3 drop by drop, until a clear, colourless solution remained.

Step 4. The tube was cooled, and the acid solution was then carefully diluted with about 10 mls water. Conc. NH_4OH was next added, until the solution was alkaline, and a colourless precipitate of $Zr(OH)_4$ was obtained. This was separated by centrifugation and washed with two 10 ml portions of water.

Step 5. As step 8 of Procedure 1.

Mandelic acid has been found[46,47] to be a specific reagent for the precipitation of zirconium, and provided care is taken to remove any free acid by thorough washing, the direct weighing of the precipitate may reliably be used to estimate the yield.[45]

After the zirconium sources had been prepared by one of the methods described above, they were counted in the usual way. The activity of these sources reached a maximum, due to the growth in them of the 74m ^{97}Nb, about 7 hours after the last zirconium precipitation, and thereafter they decayed with the expected 17 hour half-life, showing no sign of any contaminating activity. The results are shown in Table VII.

(e) MOLYBDENUM

The yield of ^{99}Mo was determined: the decay chain for this mass-number being[35]:-

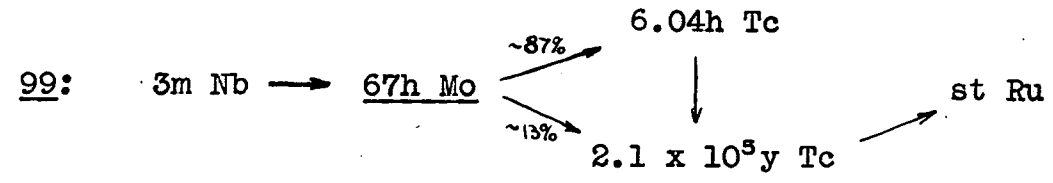

The method used in separating molybdenum from the mixed fission-products was a modified form of that reported by Ballou.[48]

A suitable carrier solution, containing approx. 10 mg Mo/ml as $(NH_4)_2MoO_4$, was prepared by dissolving about 3 g MoO_3 in 250 mls of 2N NH_4OH. This was standardized by a gravimetric method described by Vogel.[49] Molybdenum "oxinate" was precipitated by the addition of 8-hydroxyquinoline (oxine), and the precipitate was filtered off and weighed, after being washed with hot water, ethanol, and ether, and dried in a vacuum-desiccator.

Procedure:-

Step 1. 1 ml of the standardized molybdenum carrier solution, 1 ml of saturated oxalic acid solution, and 6 mls of 5M HNO_3, were added to a 20 ml aliquot of the stock solution, or to the uranyl nitrate solution used in the work on the Xenon isotopes (see chapter 5). The molybdenum was then precipitated by the addition of 5 mls of 2% alcoholic α-benzoinoxime solution. After stirring the solution and then allowing it to stand for two minutes, it was centrifuged. (Because of the small difference in density between the two phases, prolonged centrifuging was required, and the supernate had to be carefully removed by means of the apparatus shown in Fig IV). The precipitate was washed with 20 mls of 1M HNO_3.

Step 2. 2 mls of conc. HNO_3 and 1 ml 70% $HClO_4$ were added

to the molybdenum precipitate. The mixture was heated carefully until the precipitate dissolved, and heating continued until copious $HClO_4$ fumes were evolved. The solution was then cooled, and 20 mls of water were added, followed by 2 mls conc. NH_4OH. Any precipitate which formed at this stage was disregarded. 1 ml of iron carrier solution, containing 5 mg Fe as $FeCl_3$, was added, and after stirring, the precipitated $Fe(OH)_3$ was removed by centrifugation.

Step 3. 6 mls of 5M HNO_3 were added to the supernate from step 2, and the precipitation of the molybdenum was repeated by the addition of 5 mls of the α-benzoinoxime solution. The precipitate was separated by centrifugation, and washed with 20 mls of 1M HNO_3.

Step 4. Step 2 was repeated, but without the addition of the iron carrier solution. Any organic residue was filtered off.

Step 5. The solution from step 4 was rendered just acid to methyl red (pH=5) by the addition of a few drops of 2M H_2SO_4. 5 mls of 2M ammonium acetate were then added, and the solution was diluted to 50 mls and heated to about 90°C. The molybdenum was then precipitated by the addition of a freshly prepared 3% solution of oxine in dilute acetic acid - sufficient to turn the supernate perceptibly yellow. The solution was kept hot until the precipitate coagulated, then it was centrifuged, and the precipitate was washed with 20 mls of hot water. The molybdenum oxinate was then

transferred to a weighed filter-paper in the filter-stick, washed again with hot water, then with ethanol and ether, and dried, weighed, and mounted for counting in the usual way.

The sources prepared in this way decayed with the expected 67 hour half-life, and showed no sign of any contaminating activity. The results are shown in Table VIII.

(f) ANTIMONY

The yield of ^{129}Sb was determined: the decay chain for this mass-number being:-

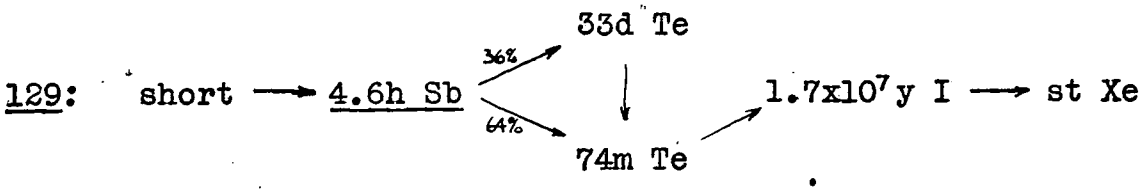

The initial separation of the antimony from the mixed fission-products was made by the solvent extraction method of White and Rose,[50] and the final precipitation, for gravimetric determination of the recovered carrier, was of antimony pyrogallate.

A suitable antimony carrier solution, containing approx. 10 mg Sb/ ml as $SbCl_3$, was prepared and standardized as pyrogallate by the method described by Boldridge and Hume.[51]

Procedure:-

Step 1. 1 ml of the standardized antimony carrier solution,

and 10 mls of conc. HCl, were added to a 20 ml aliquot of the stock solution. This mixture was evaporated down on a hot-plate, with the addition of more HCl from time to time, until all the HNO_3 had been removed.

Step 2. The solution was made up to 15 mls, 5M with respect to HCl. A solution of $KMnO_4$ were added, oxidising Sb(III) to Sb(IV), drop by drop until the purple colour just persisted. (This was easily visible above the strong yellow colour due to the presence of UO_2^{++}). The excess $KMnO_4$ was then destroyed with a few drops of 0.1% $NH_2OH.HCl$.

Step 3. The solution was transferred to a small separatory funnel, and about 0.4 g each of oxalic and citric acids were added. The mixture was stirred mechanically until the solids had dissolved, and then the antimony oxalate-citrate complex was extracted into two 20 ml portions of ethyl acetate. The organic layers were collected in a large centrifuge tube.

Step 4. The tube was placed in a hot water-bath and the ethyl acetate was evaporated off. Just before reaching dryness, 2 mls conc. HCl were added to the solution, and it was transferred to a small centrifuge tube. After dilution to 10 mls, the solution was saturated with H_2S, centrifuged, and the precipitate of Sb_2S_3 was washed with water.

Step 5. The precipitate was dissolved in 2 mls of warm conc.

HCl, and any insoluble residue (S) was removed by centrifugation. The clear solution was transferred to a large pyrex centrifuge tube.

Step 6. The solution was carefully evaporated almost to dryness, and then diluted to about 5 mls. If SbOCl was precipitated, a few drops of conc. HCl were added until it dissolved. 1 ml of 6% H_2SO_3 was added, and the solution heated almost to boiling point. After cooling, another ml of 6% H_2SO_3 was added, and the solution again heated. All the antimony was now present in the tri-valent state.

Step 7. After cooling, 0.2 g sodium acid tartrate was added, and the solution was diluted to 10 mls. 10 mls of a freshly prepared solution of pyrogallol (0.3 g in 10 mls water) were then added, precipitating the antimony as pyrogallate. This precipitate was separated by centrifugation, and thoroughly washed, to remove any occluded free pyrogallol, with two 10 ml portions of water. It was then slurried with ethanol, and transferred to a weighed filter-paper disc in the filter-stick. This was washed with more ethanol, and ether, before being dried, weighed, and mounted for counting in the usual way.

The activities of the sources prepared in this way reached a maximum about 3 hours after the final antimony extraction, due to the growth in them of the 74m ^{129}Te. Some unidentified long-lived activity was observed to be present, but there was

no difficulty in resolving the decay curves obtained to determine the activity due to the 4.6h ^{129}Sb. The results are shown in Table XV.

(g) RUTHENIUM (Summary)

The yield of ^{105}Ru was determined: the decay chain for this mass-number being[35]:-

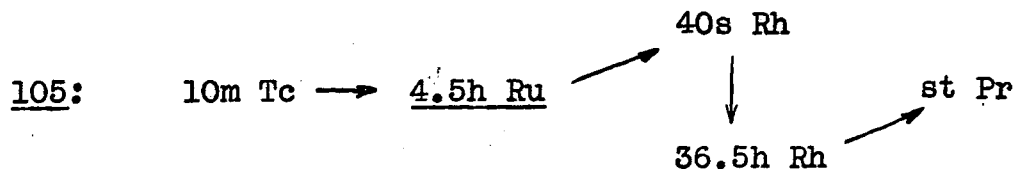

The ruthenium samples were prepared by R.H. James, using the procedure devised by Glendenin.[52] Direct separation of ruthenium from the mixed fission-products was achieved by distillation of the volatile RuO_4, following oxidation of the ruthenium chloride carrier with $HClO_4$. The volatilized RuO_4 was absorbed in NaOH solution and then reduced with ethanol; the precipitated ruthenium oxides were dissolved in HCl, and the ruthenium metal was precipitated by reduction with magnesium metal. These precipitates were washed, dried, and mounted for counting in the usual way.

The results are reported in Chapter 6, and shown in Table IX.

(h) PALLADIUM (Summary)

The yields of ^{109}Pd, ^{111}Pd and ^{112}Pd were determined:

the decay chains for these mass-numbers being:-[35]

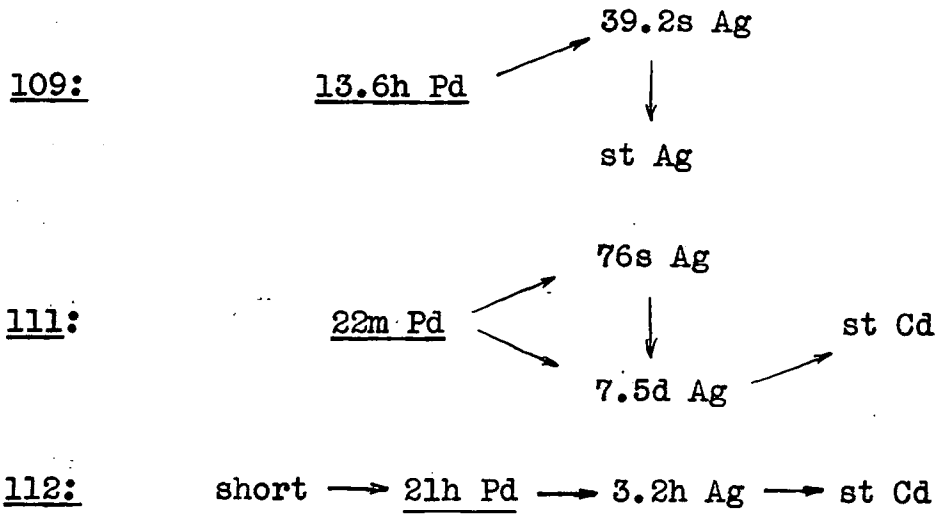

The palladium samples were prepared by R.H. James, using the procedure described by Glendenin.[53] Direct separation of palladium from the mixed fission-products was achieved by precipitation of palladium dimethylglyoxime from an aliquot of the stock solution, made 0.4M with respect to HNO_3. After scavenging with $Fe(OH)_3$ and AgI, the palladium was finally precipitated, weighed, and mounted for counting, as palladium dimethylglyoxime.

When the yield of 22m ^{111}Pd was to be determined, the separation was started as quickly as possible after the end of the irradiation, which was always short to prevent the build-up of the longer-lived nuclides. When determining the yields of ^{109}Pd and ^{112}Pd, however, the ^{111}Pd was permitted to decay before the separation was started, so that the 7.5d ^{111}Ag would not be present in the palladium samples.

The results for these nuclides are reported in Chapter 6, and are shown in Tables X, XI A, and XII.

(i) SILVER (Summary)

The yields of ^{111}Ag, ^{113}Ag, and ^{115}Ag were determined: the decay chains for these mass-numbers being[35]:-

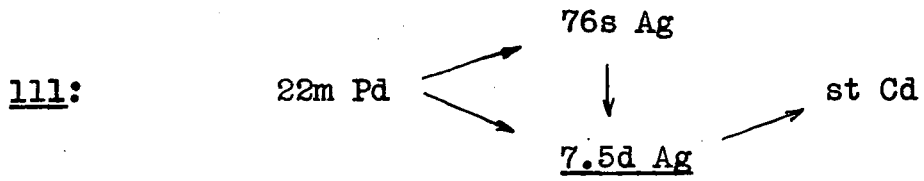

The silver sources were prepared by R.H. James, using the procedure described by Glendenin.[54] Separation of silver from the mixed fission-products was achieved by the precipitation of silver chloride with dilute HCl. (The supernate was then taken for the barium separation: see page 25). After alternately scavenging with $Fe(OH)_3$, and precipitating Ag_2S from an ammoniacal solution, the silver was finally precipitated, and weighed and mounted for counting, as silver chloride.

When the yield of ^{115}Ag was to be determined, the separation was started as quickly as possible after the end of the irradiation, which was always short to prevent the

build-up of the longer-lived nuclides. When determining the yield of ^{111}Ag, however, sufficient time had to be allowed for the decay of its parent 22m ^{111}Pd before beginning the separation.

The results for these nuclides are reported in Chapter 6, and are shown in Tables XI B, XIII, and XIV.

(j) CERIUM (Summary)

The yield of ^{143}Ce was determined: the decay chain for this mass-number being:-

143: 19m La ⟶ 32h Ce ⟶ 13.7d Pr ⟶ st Nd

The cerium sources were prepared by R.H. James, using a method based on that due to Warf.[41] Cerium (III) was oxidised with $KBrO_3$ and extracted into T.B.P. (tri-n-butyl phosphate), and then back-extracted into an aqueous solution by reduction with H_2O_2. The cerium was finally precipitated, and weighed and mounted for counting, as cerous oxalate.

Sufficient time was allowed, before beginning the extraction, for the 19m ^{143}La precursor to decay.

The results are reported in Chapter 6, and are shown in Table XVIII.

CHAPTER 4

MISCELLANEOUS EXPERIMENTAL WORK

Part 1 The Effect of the D + D Neutrons

As was stated in Chapter 2, D + D neutrons are inevitably produced by the neutron-generator, due to the bombardment of deuterium deposited in the target by the deuteron beam itself.

The reaction may be represented by the equation:

$$^{2}H\ (D) + {}^{2}H\ (D) \longrightarrow {}^{3}He + {}^{1}n + 3.28\ MeV$$

For a deuteron beam of 200 keV and a thick D_2O target, Hanson et al.[32] report a yield of about 3×10^{7} neutrons per sec. per micro-ampere. The neutron energy depends on the angle of emission, but is in the region of 2.5 MeV.

Measurements were made to assess the contribution to the fission-yields from fission caused by these neutrons.

For this purpose, a blank zirconium target was fitted to the neutron-generator, and four packets, each containing 10 g of U.N.H. were strapped underneath. The deuteron beam was then focussed on to the target, and the bombardment continued for 5 hours. During this period, the beam-current remained at 200 μa., but the neutron-monitor, being biassed to count only 14-MeV neutrons, recorded none of the lower-energy neutrons produced.

After the irradiation had continued for two hours, the first U.N.H. packet was removed from the target-block, and was analysed in the usual way to determine the fission-produced silver (by R.H.J.) and barium (by D.J.S.) activities. The remaining packets were removed at hourly intervals until the end of the irradiation, and were similarly analysed.

The four barium samples which were produced all had initial activities, when corrected for decay, chemical yield, etc., of about 10^3 c.p.m., and they decayed with the 85-minute half-life appropriate to ^{139}Ba. Any 12.8-day ^{140}Ba which may have been present was of much too low intensity to be reliably measured.

The silver samples, on the other hand, were virtually inactive, giving perhaps 20 c.p.m. above the background of 40 c.p.m.

The fact that the longer-irradiated samples showed no significant increase in the amount of ^{139}Ba produced suggests that deuterium builds up fairly rapidly on the target-block, to a saturation level, though, because the geometry of the system was altered to some extent as each U.N.H. packet was removed, no more quantitative interpretation can be made.

The ^{139}Ba activity in U.N.H. samples of comparable weight, irradiated for similar periods with neutrons from normal zirconium-tritium targets, was almost always higher than

5×10^4 c.p.m. (see Table III). It would therefore seem that the D + D neutrons cannot account for more than about 2% of the total ^{139}Ba yield.

The D + D neutron fission-yield in the region of the central "trough" is evidently, from the observed silver sample activities, even smaller than it is for D + T neutrons. (As would be expected, for lower energy fission). For this reason, and since only relative measurements were made, the over-all error due to D + D neutrons should not be more than 2% at any point.

Part 2 The Sellotape Absorption Factors

In order to calculate the fission-yield of a given nuclide, its absolute activity in each source must be known. This can be obtained by dividing the observed activity by a number of correction factors, amongst them being one for absorption in the layer of sellotape with which, for the purposes mentioned in the previous chapter, the sources were covered.

It was frequently possible to measure the required sellotape absorption factors directly, by preparing samples containing the appropriate nuclide, and counting them in the 2π-counter first without, and then with, a sellotape covering.

In the case of the two longer-lived nuclides (67h ^{99}Mo, and 12.8d ^{140}Ba) suitable samples were prepared from the fission-products in a portion of pile-irradiated UO_3, using the separation procedures described in the previous chapter. The iodine samples were made from a stock-solution of 8d ^{131}I which was available at that time. For the shorter-lived nuclides, however, the samples used were those which had actually been prepared for yield-measurement purposes.

Once a suitable sample had been prepared, it was placed, uncovered, on the slide of the 2π-counter, and was then pushed into the counting position, very slowly and carefully, so as not to displace the O-ring. The counter was then

left to flush, with the gas flowing at its normal rate (0.6 ml/sec.).

The scaler settled down to a steady counting rate when the counter had been adequately flushed, but measurements were not started for a further five minutes. (The total time between putting a source into the counter and beginning to count was generally about 15-20 minutes). In the case of the long-lived nuclides, which decayed negligibly during the course of the experiment, measurements were repeated two or three times (about 10,000 counts being recorded each time, to keep the statistical error to a minimum) and the mean value was taken. For the shorter-lived nuclides, however, careful note was taken of the time of each reading, and sufficient readings were taken to be sure they lay on a decay-curve of the appropriate half-life. (e.g. in the case of 85m ^{139}Ba, six two-minute readings were taken over a period of 20 minutes).

The sample was then removed from the counter, covered by a layer of sellotape, and replaced. The counter was then flushed rapidly, by increasing the gas flow-rate for a few moments, before a similar series of measurements were recorded. The counting-rates were corrected for decay, when appropriate, and then the ratio:

$$\frac{\text{c.p.m. for sample covered by 1 layer of sellotape}}{\text{c.p.m. for uncovered sample}}$$

was the required sellotape absorption factor.

The measurements on the ^{97}Zr + ^{97}Nb and ^{129}Sb + ^{129}Te samples, where parent and daughter have similar absorption characteristics, were not made until radioactive equilibrium had been reached. ^{140}Ba - ^{140}La presented a special case, and is discussed in the next part of this chapter.

In some cases, however, it was not possible to prepare samples in which only one radioactive species was present (e.g. the bromine samples always contained both 2.3h ^{83}Br and 32m ^{84}Br whenever their specific activities were high enough for reliable absorption measurements; similarly, the yttrium samples invariably contained shorter- and longer-lived isotopes in addition to the 10h ^{90}Y) and so the factors for these nuclides had to be estimated from consideration of their β-energies, and by interpolation from measured data.

R.H. James[55] has shown, by comparison of the sellotape and aluminium absorption curves for $Ag^{131}I$ samples in the 2π-counter, that a single layer of sellotape is equivalent to a thickness of 10 mg/cm^2 of aluminium. In addition, Cuninghame et al.[56] have published aluminium absorption curves for ^{83}Br and ^{105}Ru samples measured in a 4π-counter, and, since these would not be expected to be very different for a 2π-counter, the sellotape absorption factors for these two nuclides were therefore estimated by combining the two sets of results.

Table I shows the sellotape absorption factors for the nuclides met in this work, arranged in order of decreasing β-energy.

TABLE I

The Sellotape Absorption Factors for Nuclides in the 2π-Counter

NUCLIDE	MAXIMUM β-ENERGY. (MeV)	SELLOTAPE ABSORPTION FACTOR	HOW DETERMINED (*)
^{84}Br	4.68	0.95	I
^{93}Y	3.1	0.91	I
^{115}Ag	3.0	0.90	I
^{139}Ba	2.38	0.87	M
^{111}Pd	2.13	0.85	I
^{113}Ag	2.1	0.85	M
^{97}Zr + ^{97}Nb	1.91 + 1.27	0.82	M
^{129}Sb + ^{129}Te	1.87 + 1.45	0.70	M
^{143}Ce	1.39	0.79	I
^{99}Mo	1.23	0.77	M
^{105}Ru	1.15	0.65	C
^{111}Ag	1.04	0.70	I
^{140}Ba	1.02	0.62	Mx
^{109}Pd	0.99	0.68	I
^{83}Br	0.94	0.66	C
^{131}I	0.61	0.63	M
^{112}Pd + ^{112}Ag	0.28 + 4.1	0.66	I

(*) M = Measured

I = Interpolated

x = Special case, see Part 3

C = From the combined results of James[55] and Cuninghame et al.[56]

Part 3 The Growth Curve for $^{140}Ba - ^{140}La$

When a radioactive parent and daughter reach equilibrium, if both have similar absorption characteristics, the parent activity can be obtained from the observed total activity by dividing by a factor calculated from the decay constants. Of the nuclides met in this work, ^{97}Zr-^{97}Nb and ^{129}Sb-^{129}Te come into this category.

In the case of ^{140}Ba-^{140}La, however, a number of conversion electrons are emitted, and it is not possible simply to use a calculated correction factor in order to determine the ^{140}Ba activity.

To overcome this difficulty, therefore, a growth curve was determined by mounting initially daughter-free samples of ^{140}Ba, and observing the growth of ^{140}La in them, and from this curve the required correction factor could be obtained.

For this purpose, ^{140}Ba was isolated from the fission-products in a sample of pile-irradiated UO_3 (which was sufficiently aged for all the 85m ^{139}Ba to have decayed) using the procedure described in the previous chapter, and the resulting $BaCl_2$ precipitate (about 10 mg) was dissolved in 100 mls of water to make a stock-solution.

Portions of this solution, to each of which about 10 mg of barium carrier were added, were then scavenged by repeatedly precipitating LaF_3 from them (by addition of HF

followed by 3 x 5 mgs of La carrier). The time of the last LaF_3 precipitation was noted, and then the barium was precipitated as $BaCl_2.H_2O$, mounted, dried, weighed, and placed in the 2π-counter with no sellotape covering, as rapidly as possible. After counting the sample just long enough to ensure statistical accuracy, the sample was covered with a layer of sellotape and then counted once more. The total time which elapsed between the final removal of the daughter La activity, and the first measurement on the source covered by sellotape, was never more than about 90 minutes, which was short compared with the half-lives of the two nuclides being studied.

The growth, and eventual decay, of the activity of each of the samples so prepared was then followed, and curves were obtained such as that shown in Fig. V. The results are summarised in Table II.

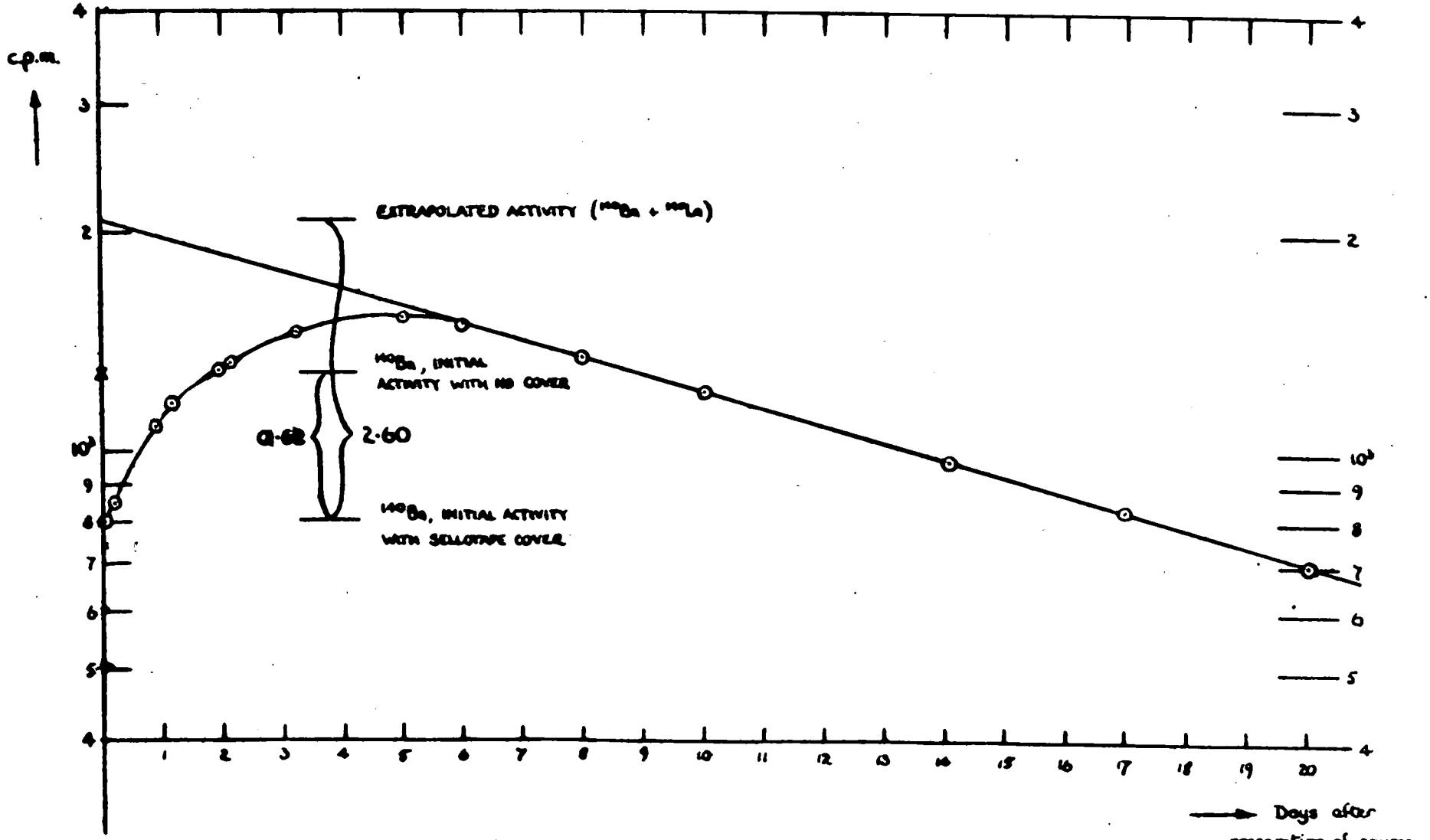

FIG. V: GROWTH CURVE FOR ^{140}Ba - ^{140}La.

TABLE II

The Sellotape Absorption, and Daughter Activity Factors for ^{140}Ba

Source Number:	1	2	3	Mean
Weight (*), mg:	16.2	17.2	16.0	--
Initial Activity c.p.m.:				
(a) No sellotape	$1.29 \cdot 10^3$	$1.25 \cdot 10^4$	$1.22 \cdot 10^4$	--
(b) 1 layer sellotape	$8.00 \cdot 10^2$	$7.74 \cdot 10^3$	$7.55 \cdot 10^3$	--
Extrapolated Activity, c.p.m. (c):	$2.08 \cdot 10^3$	$2.00 \cdot 10^4$	$1.95 \cdot 10^4$	--
Sellotape Absorption Factor (b/a):	0.620	0.619	0.624	0.62
Daughter Activity Factor (c/b):	2.60	2.59	2.60	2.60

(*) The samples were not of the same specific activity.

CHAPTER 5

THE DETERMINATION OF THE YIELDS OF TWO XENON ISOTOPES

Part 1 Summary

Epstein[57] has described a method whereby the stable isotopes of krypton and xenon produced in fission may be isolated, prior to determining their relative yields mass-spectrometrically. He took solid samples of irradiated uranium, which had to be dissolved up, in a special apparatus, to liberate the fission gases.

If one wishes to compare the yields of some active rare-gas isotopes with those of other fission-products in the same sample, Epstein's method has the disadvantage that one cannot be certain that none of the active rare-gas is lost by diffusion before the sample is safely inside the dissolving apparatus.

This difficulty can be overcome, however, by irradiating the uranium, preferably already in solution, inside a sealed vessel, and by adding beforehand a small amount of gas to act as a carrier, so that the amount which is finally recovered may be measured.

The heavier fission-produced krypton isotopes are all very short-lived, whilst the half-lives of the lighter ones, which occur in lower yield, (114m ^{83m}Kr; 4.4h ^{85m}Kr; 78m ^{87}Kr;

2.8h ^{88}Kr) are all so similar that it would be difficult, if not impossible, to resolve the decay curve of a mixture of these species. Two xenon isotopes, ^{133}Xe and ^{135}Xe, on the other hand, have half-lives of the right order, yet differing sufficiently, to make a radiometric determination of their fission-yields possible.

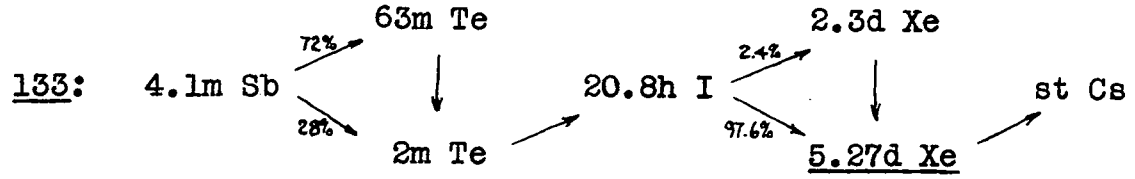

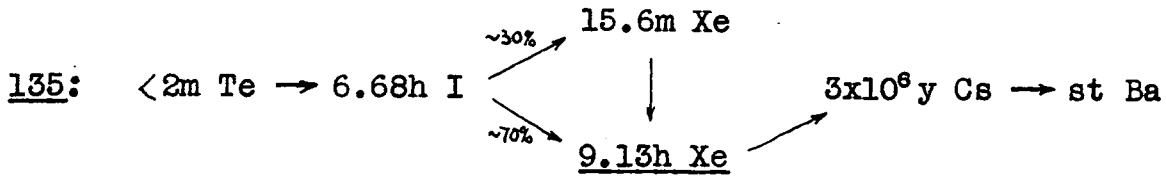

A special apparatus was therefore built which enabled these xenon isotopes to be isolated from the other fission-products, including the long-lived kryptons. This apparatus is shown in Fig. VI, and it consists essentially of three parts:

(i) a detachable glass vessel in which a uranyl nitrate solution can be irradiated. (This is shown in greater detail in Fig. VII).

(ii) a section for purifying the recovered xenon. (Shown on the right-hand side of Fig. VI).

(iii) a counter-filling section. (Left-hand side of Fig. VI).

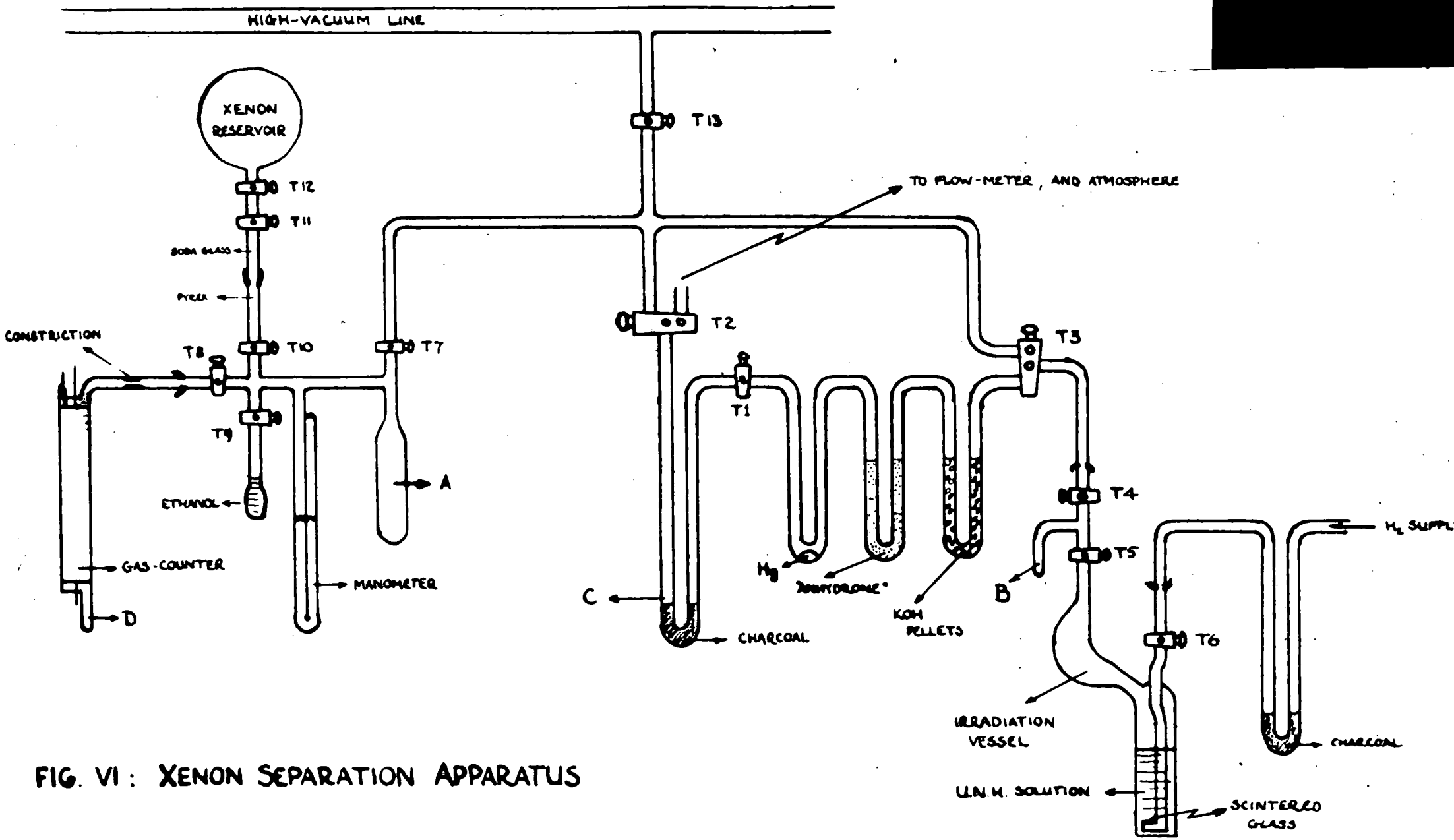

FIG. VI : XENON SEPARATION APPARATUS

Preliminary experiments showed that xenon itself could be used satisfactorily as a counter filling gas. After purification therefore, the active xenon, together with the required amount of inactive gas and ethanol as an internal quenching agent, was sealed up in a gas-counter, and its decay was followed. As was expected, no difficulty was experienced in resolving the decay-curves so obtained into their 9.1-hour and 5.3-day components.

In order to correlate the xenon results with those already obtained for other nuclides, molybdenum was separated from the same irradiated solutions, and the activity of the 67-hour ^{99}Mo was measured in the 2π β-proportional counter used in the previous experiments. A comparison of the efficiencies of the two counters was later obtained by measuring the xenon and molybdenum yields produced by slow-neutron fission, and by making use of the well-established published values for these yields.

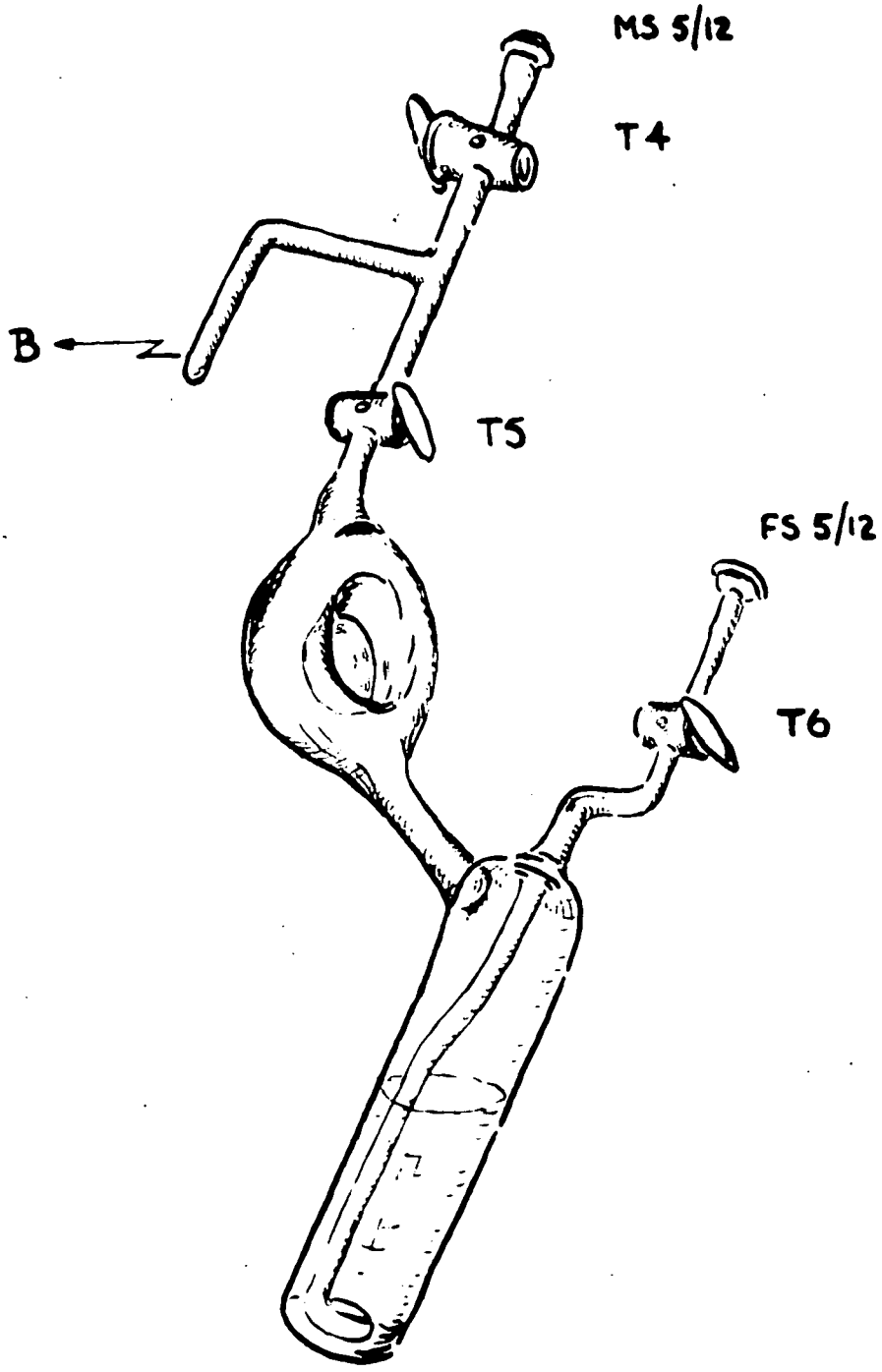

FIG VII : IRRADIATION VESSEL

Part 2 Preparation for the Irradiations

A solution containing 24 g of U.N.H. in about 60 mls of water was freed from any radium daughter activity present (see part 5a) by repeated $BaSO_4$ precipitations, as has already been described (Chapter 2, part 3), and was then introduced into the irradiation vessel. A small amount of molybdenum carrier (1 ml of standardized $(NH_4)_2MoO_4$, containing about 0.2 mg Mo) was added at this stage to prevent the fission-produced molybdenum from adhering to the walls of the vessel after the irradiation.

The irradiation vessel was then clipped on to the vacuum-apparatus, by means of its hemi-spherical joints, in the position indicated in Fig. VI and the next step was to flush the air out of both the irradiation vessel and the xenon recovery section of the apparatus.

This was achieved by passing a steady stream of hydrogen, at about 0.5 ml per sec., first through a trap containing charcoal at liquid N_2 temperature to remove any condensible impurities, then into the apparatus through T6 and the scinter in the irradiation vessel, through the uranium solution, next through part of the apparatus by way of taps T5, T4, T3, T1, and T2, and finally through a flow-meter and out into the atmosphere.

During this process, the charcoal trap C was immersed

in a water-bath at about 60°C, to remove any adsorbed impurities. After about an hour, the apparatus having been flushed sufficiently, the hydrogen flow was stopped, care being taken to close tap T2 first, to prevent air from getting back into trap C.

In the meantime, the gas-counter and the counter-filling part of the apparatus were pumped down, and then, with taps T7, T8 and T9 closed, a little xenon was allowed into the bulb A from the xenon reservoir, through taps T12, T11 and T10. The total volume of this section of the apparatus was about 60 mls, and for carrier purposes this was filled with xenon to a pressure of about 3 cms Hg. At room temperature, this was equivalent to about 12 mg of xenon. The pressure of the gas in A was measured by means of the mercury manometer, and this pressure, and the room temperature were both recorded.

The hydrogen was next pumped out of the section of the apparatus between taps T3 and T5, and then, by closing T13 and opening T7, the xenon could be transferred from the bulb A to the side-arm B on the irradiation vessel, by immersing B in liquid nitrogen. When the manometer showed zero pressure, the xenon had entirely condensed in B, and taps T4, T3 and T7 were closed.

The irradiation vessel was now removed from the rest of the apparatus; B was warmed to room temperature, and on opening T5 the xenon was enabled to diffuse into the bulk of

the vessel.

By tipping the vessel to a horizontal position, the solution inside poured into the hemispherical-shaped middle portion, which had been specially made to fit snugly round the target block of the neutron-generator to ensure the best possible geometry was achieved during the irradiations. These were carried out in the usual way, neutron-monitor readings being recorded at 10-minute intervals throughout.

At the end of the irradiation (4 hours duration in Run 21, 3.5 hours in Run 22) the irradiation vessel was put back on the vacuum apparatus, and the connecting section, between taps T3 and T4, was pumped down. The xenon separation was not begun until approximately 12 hours had elapsed from the end of the irradiation, however, thereby allowing the xenon activities to build up, as a result of the decay of their comparatively long-lived precursors. (cf. the decay-chains on page **60.** . The ^{135}Xe reaches maximum activity about 11 hours after the irradiation).

Part 3 Isolating the Fission-Produced Xenon

The procedure for recovering the xenon carrier gas, together with the active fission-produced xenon, from the irradiated uranium solution, was similar to that which has been described for preparing the solution for irradiation.

Purified hydrogen was blown steadily through the solution, at not more than 0.5 ml per sec., and this carried the xenon through traps containing first, KOH to remove acid spray; second, "Anhydrone" ($Mg(ClO_4)_2$) to dry the gas; and third, a little mercury, warmed to increase its vapour-pressure by means of a very small flame, to remove all possible traces of iodine.

The gas then passed through the charcoal trap C, which was immersed in an acetone-alcohol bath, kept at -20°C by the occasional addition of small pieces of solid CO_2. Arrol, Chackett, and Epstein[58] have shown that xenon may be adsorbed on charcoal at this temperature, whilst krypton is not adsorbed. The long-lived krypton isotopes therefore pass on with the hydrogen stream, through the flow-meter, and out into the atmosphere.

Preliminary experiments showed that all the xenon carrier gas could be transferred from the irradiation vessel to trap C in under 15 minutes, by a stream of hydrogen passing at 0.5 ml per sec. The hydrogen stream was therefore stopped after 15 minutes, and the time was carefully noted: this

was taken as the time for the last separation of the xenon isotopes from their iodine precursors.

The rest of the apparatus having previously been pumped down, taps T1, T3, and T7 were closed and T13 was opened, after which T2 was also slowly opened (C being maintained at -20°C) until all the hydrogen had been pumped out of C. Tap T13 was then closed, and the cold bath around trap C was replaced by a water-bath, raising its temperature to about 40°C. On opening tap T7 (T8, T9, T10 being closed) and immersing bulb A in liquid nitrogen, the xenon distilled from C to condense in A.

Less than ten minutes was required for this operation. If the hydrogen had not previously been completely removed from trap C, it could now be detected by a positive reading on the manometer, and pumped away at this stage.

Once the manometer was reading zero pressure, tap T7 was closed, and A was allowed to warm up to room temperature. The pressure of the recovered xenon was obtained from the manometer reading, and was recorded together with the room temperature. It was now possible to calculate the fraction of the xenon carrier gas which had been recovered. The difference in volume associated with the two manometer readings, due to the mercury standing at slightly differing heights, was always very small (less than 0.6% of the total volume in every case) so no correction was made

for its effect on the calculated xenon recovery.

Once the xenon separation had been completed, a further 10 mg of molybdenum carrier was added to the uranium solution in the irradiation vessel and the fission-produced molybdenum was then isolated. Its activity was determined in the 2π-β-proportional counter used in the previous experiments.

For this part of the work, ^{99}Mo was chosen as a reference nuclide (85m ^{139}Ba being too short-lived for this purpose) both because it has a suitable half-life (67-hours) and occurs in high yield, and also because molybdenum could very easily be separated from the large volumes of uranyl nitrate solution which were used, by the method which was described in Chapter 3.

Part 4 The Gas-Counter

After some unsuccessful trials with a home-made gas-counter, a commercial tube was used in these experiments. This had a 100 μ diameter tungsten anode, and a passive-iron cathode. Its total volume was about 90 mls, of which about 70 mls was the actual cathode volume.

A suitable filling for this counter was obtained by filling the bulb A with xenon and ethanol, at pressures of 10 and 2 cms. Hg respectively, and then condensing these gases in the counter by opening tap T8 and immersing the side-arm D in liquid nitrogen. The counter could then be sealed at the constriction G, and removed from the filling apparatus at this point. The total pressure inside the counter (when D was once more at room temperature) was thus, approximately, $(10+2)\times 60/90 = 8$ cms. Hg.

The counter was placed inside a lead castle, and connected to the electronic equipment shown in the block diagram in Fig. VIII.

No references to the previous use of xenon as a counter-filling gas have been found, save one (Wilkinson[59]) which reports that the noble gases are very unsuitable for proportional and Geiger counters because of the metastable states, of about 10^{-4} sec. life-time, which are formed in them. However, by modifying the standard Type 1014A Probe Unit to

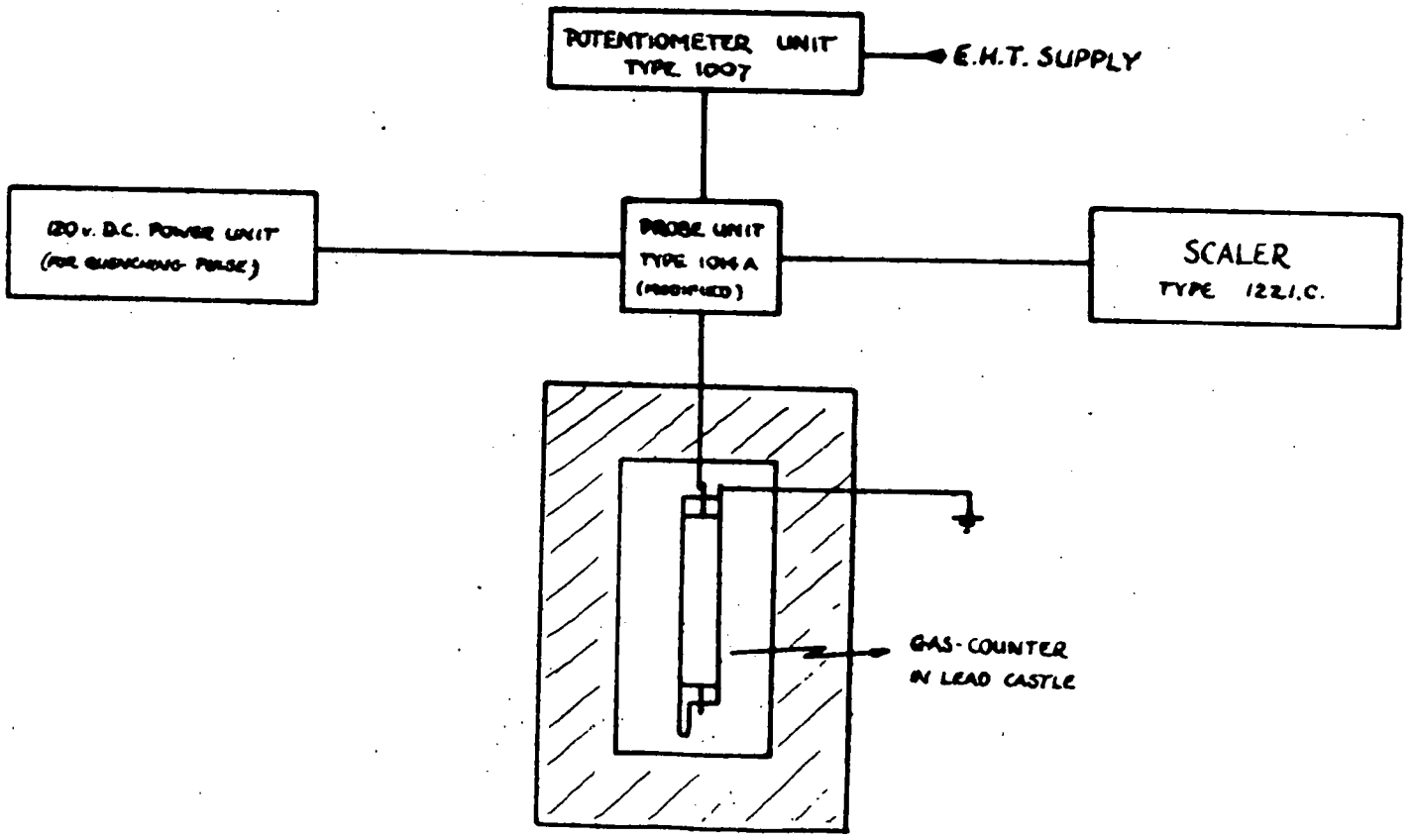

FIG. VIII : ELECTRONIC EQUIPMENT ASSOCIATED WITH THE GAS-COUNTER.

increase the quenching pulse (by 120V) and the paralysis time (to 840 μ sec.), perfectly satisfactory results have been obtained.

Using an external γ-source, the threshold voltage for counting was about 1350V., above which a plateau was obtained, at least 200V long, with a slope of less than 2% per 100V. The background count, taken at 1450V, was always about 50 c.p.m.

Because it was necessary to follow the decay of the active xenon for long periods, during which a tap may possibly have become "streaky", the counter was sealed up each time it was filled. The drawback in this was that the background count could not be determined, other than immediately before and after the counter had been filled with the active gas. Fortunately, however, this did not lead to any serious error, since the xenon activity was in general at least an order of magnitude greater than the background.

Part 5 (a) The Detection of ^{226}Ra in the Commercial U.N.H.

In the course of preliminary experiments on the xenon recovery procedure, the presence of a significant amount of 1622y ^{226}Ra (a decay-product of ^{238}U) was detected in the commercial uranyl nitrate.

The gas-counter was, at one stage, filled with xenon which had been in contact with an un-irradiated solution of the uranyl nitrate, and this filling was found to be active. Furthermore, its activity increased from about 500 to 700 c.p.m. over a period of two hours.

On quickly replacing this "active" filling with a new "inactive" one (the counter being fitted with a tap at this time) some active material was observed to remain behind in the counter. This gave initially, about 200 c.p.m., and decayed with an apparent half-life of about 35 minutes.

The entire procedure was repeated, with the same result, after the counter had first of all been filled afresh, to check the background, and that the xenon and ethanol reservoirs had not in some way become contaminated.

These observations suggested that there might be a significant amount of ^{226}Ra present in the original solution, since this decays to 3.8d ^{222}Rn, which would follow xenon into the gas-counter. The observed increase in activity would be due to the growth of the active daughters of this

nuclide, and these, not being gaseous elements, would remain in the counter when the original filling, with the radon, was removed. Further, the daughters of ^{222}Rn are known to decay with an apparent half-life, measured over a short period, of about 30 minutes.

When the experiment was repeated once more, but with a uranyl nitrate solution which had been freed from radium by repeated $BaSO_4$ precipitations (see Chapter 2, Part 3), the recovered xenon was completely inactive.

(b) The Fast-Neutron Bombardment of Xe and Mo Carriers

The effect of fast-neutron bombardment on the xenon and molybdenum carriers was also investigated in a preliminary experiment.

The irradiation vessel was filled with 70 mls of water, and 10 mg Mo carrier and 20 mg Xe carrier were added. (2 mg Mo and 12 mg Xe were the quantities usually taken). The vessel was then fixed to the neutron-generator and irradiated for four hours, and immediately afterwards the xenon and molybdenum were isolated in the usual way.

The molybdenum proved to be completely inactive, but the xenon gave, initially, about 300 c.p.m. This xenon activity, however, decayed with a half-life of about 140 minutes, and

there was no trace of any longer-lived activity.

It was thus apparent that no correction had to be applied for the interaction of the 14-MeV neutrons with the carrier xenon or molybdenum which was present in the uranyl nitrate irradiations.

(c) The Slow-Neutron Irradiation

In order to correlate the xenon results with those obtained for the other nuclides, it was necessary to calibrate the gas-counter with respect to the 2π-counter. This was achieved by measuring, in the usual way, the activities of the ^{133}Xe and the ^{99}Mo produced in the slow-neutron fission of the ^{235}U present in natural uranium, and by making use of the well-established published yields for these nuclides. (See Chapter 6 for the calculations involved).

The neutron source which was used consisted of a 1 g. radium-beryllium capsule and two 1 g. antimony-beryllium capsules, (both of the latter, however, were very much below their saturation activity).

The irradiation vessel, containing about 50 g. of U.N.H. in 80 mls of solution, with xenon and molybdenum carriers as before, was strapped to the neutron-source, and the entire apparatus was immersed in a 100-gallon water tank, which

served to thermalise the neutrons.

The neutron flux was, however, very low, and it was eventually found necessary to irradiate the solution for a long period (18 days), in order to build up reasonable amounts of ^{99}Mo and ^{133}Xe. (These nuclides can both be produced by n,γ reactions, but the cross-sections for both are less than 0.5 barn. Here, however, the quantities of ^{98}Mo and ^{132}Xe present were so small, as was the neutron flux, that no measurable activity could arise from this source).

After the irradiation, the xenon and molybdenum were isolated and counted in the usual way.

The results, for all the work on the xenon isotope yields, are reported and discussed in the third part of the next chapter.

CHAPTER 6

RESULTS

Part 1 General Methods of Calculation

As was explained in chapter 2, the 14-MeV neutron-generator does not produce a steady neutron flux, and a separate allowance must be made for this in calculating the yields of each of the fission-products studied.

Let us consider an irradiation of duration T, and suppose that a fission-product is isolated at time t' after the end of the irradiation.

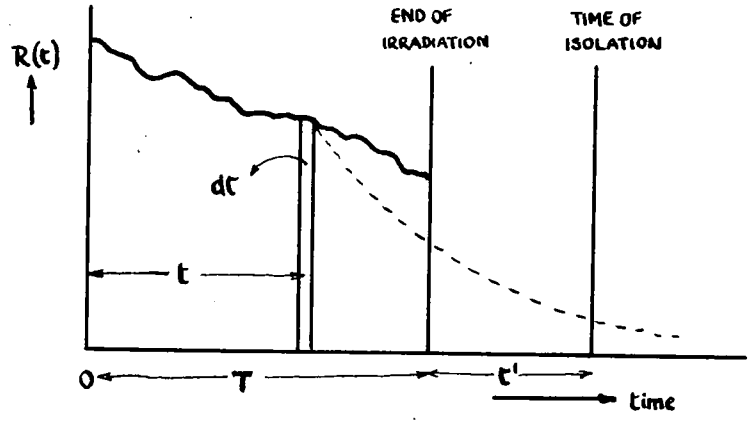

(a) Suppose that the precursors of the nuclide 1 in the chain:

$$\longrightarrow 1 \xrightarrow[\lambda_1]{} 2 \text{ (stable)}$$

are short-lived compared with T, and t', the time at which 1 is isolated.

The nuclide 1 will be produced throughout the irradiation

at an irregular rate R(t), where R is some function of time (t). During the short interval dt, the number of nuclei of 1 which are produced will be

$$dN_1 = R(t).dt$$

and these will decay exponentially, so that at the time of isolation (t') the number remaining will be

$$dN_1(t') = R(t).e^{-\lambda_1 [t'+(T-t)]}.dt$$
$$= e^{-\lambda_1 t'}.R(t).e^{-\lambda_1 (T-t)}.dt$$

Thus the total number of nuclei of species 1 present at the time of isolation will be

$$N_1(t') = e^{-\lambda_1 t'}.\int_{t=0}^{t=T} R(t).e^{-\lambda_1 (T-t)}.dt$$

Now R(t) can be expressed as

$$R(t) = B.\sigma.Y_1.\phi(t)$$

where, B = a constant for the particular irradiation under consideration. (Its value depending on the amount of uranium irradiated)

σ = fission cross-section of the irradiated nuclei.

Y_1 = fission-yield of the nuclide 1. (i.e. the percentage of fissions in which 1 is formed directly or indirectly)

$\phi(t)$ = neutron flux through the uranium sample.

But since the uranium sample and the monitor are in positions fixed with respect to the neutron-source, $R(t)$ varies in a manner proportional to the variation in the neutron-monitor counting-rate, $I(t)$,

i.e. $$R(t) = B.\sigma.Y_1.I(t) / \eta$$

where η = efficiency of the neutron-monitor, including factors relating the geometrical positions of monitor and uranium sample.

Thus:

$$N_1(t') = \frac{B.\sigma.Y_1}{\eta} . e^{-\lambda_1 t'} . \int_{t=0}^{t=T} I(t).e^{-\lambda_1 (T-t)}.dt$$

It is convenient (and results in negligible loss of accuracy, provided that the intervals taken are very much shorter than the half-life of the species concerned) to replace the integral by the summation:

$$\Sigma \, (I.e^{-\lambda_1 (T-t)}) \, \delta t \qquad \text{(abbreviated to } S_1)$$

which can then be evaluated from the recorded neutron-monitor readings, and tables of values of $e^{-\lambda_1 (T-t)}$.

An expression of this sort is valid separately for each similar nuclide investigated. Thus, if r is some reference nuclide, isolated at time t", we have:

$$\frac{N_1(t')}{N_r(t'')} = \frac{Y_1.e^{-\lambda_1 t'}.S_1}{Y_r.e^{-\lambda_r t''}.S_r}$$

the unknown factors B, σ, and η cancelling between the two expressions.

Now, by extrapolation of their decay-curves, the activities of the isolated species at the end of the irradiation, A^o, can be determined. (i.e. activities at time corresponding to t'=t"=0). Then since $A^o = c.\lambda.N^o$, we have:

$$\frac{A_1^o}{A_r^o} = \frac{c_1.\lambda_1.Y_1.S_1}{c_r.\lambda_r.Y_r.S_r}$$

or, if the detection coefficients, c_1 and c_r, are the same for both nuclides,

$$\frac{Y_1}{Y_r} = \frac{A_1^o.\tau_1.S_r}{A_r^o.\tau_r.S_1} \qquad \text{.....equation (I).}$$

where τ = 0.69315 / λ, the half-life of the species concerned.

(b) In some cases, the half-life of the immediate precursor of the isolated fission-product is not negligible compared with that of its daughter. For example, let us consider the chain:

$$\text{(short)} \longrightarrow 1 \xrightarrow{\lambda_1} 2 \xrightarrow{\lambda_2} 3 \text{ (stable)}$$

and suppose that the species 2 is isolated at time t' after the irradiation. Then, assuming that they are formed only

from the decay of 1, and are not formed directly in fission, the number of nuclei of 2 present at that time will be,

$$N_2(t') = \frac{\lambda_1}{\lambda_2 - \lambda_1} \cdot \left(e^{-\lambda_1 t'} \cdot \int_{t=0}^{t=T} R(t).e^{-\lambda_1 (T-t)}.dt - e^{-\lambda_2 t'} \cdot \int_{t=0}^{t=T} R(t).e^{-\lambda_2 (T-t)}.dt\right)$$

Once again, the integrals can be replaced by summations, and, using the same notation as in the previous paragraph, we have:

$$N_2(t') = \frac{B.\sigma.Y_1}{\gamma} \cdot \frac{\lambda_1}{\lambda_2 - \lambda_1} \cdot (e^{-\lambda_1 t'}.S_1 - e^{-\lambda_2 t'}.S_2)$$

.....equation (II).

This expression will be met again, in the discussion of the results for ^{139}Ba and ^{135}Xe.

(c) Similarly, if in the chain

$$\text{(short)} \longrightarrow 1 \xrightarrow{\lambda_1} 2 \xrightarrow{\lambda_2} 3 \xrightarrow{\lambda_3} 4 \text{ (stable)}$$

the nuclides 1 and 2 have half-lives which are not negligible relative to that of 3, and the species 3 is isolated at time t' after the end of the irradiation, the number of nuclei of 3 present at that time will be:

$$N_3(t') = \frac{B.\sigma.Y_1}{\gamma} .(C_1.e^{-\lambda_1 t'}.S_1 + C_2.e^{-\lambda_2 t'}.S_2 + C_3.e^{-\lambda_3 t'}.S_3)$$

.....equation (III).

assuming that 3 is formed only from the decay of its precursors, and is not formed directly in fission.

The factors C_1, C_2, C_3, are the Bateman coefficients:

$$C_1 = \frac{\lambda_1\lambda_2}{(\lambda_2-\lambda_1)(\lambda_3-\lambda_1)} \; ; \quad C_2 = \frac{\lambda_1\lambda_2}{(\lambda_1-\lambda_2)(\lambda_3-\lambda_2)} \; ;$$

$$C_3 = \frac{\lambda_1\lambda_2}{(\lambda_1-\lambda_3)(\lambda_2-\lambda_3)} \; .$$

This expression will be met again in the discussion of the results for ^{133}Xe.

Part 2 Results for Nuclides measured in the 2π-Counter

In order to make use of the expressions derived in part 1, it was necessary to apply corrections to the measured, extrapolated, activities of the various sources to obtain their absolute activities, and these corrections were, of course, different for the different nuclides.

The correction for absorption in the sellotape covering the sources has already been discussed (chapter 4, part 2) and corrections for daughter activities, and similar decay-scheme phenomena, will be dealt with later in connection with the individual nuclides concerned.

Correction had also to be made, however, for the self-absorption, self-scattering, and back-scattering effects in the thick samples which were used. Since these samples were all of the same diameter (1.6 cm) and were all mounted in the same way (on filter-paper discs in aluminium trays, and placed in a fixed position on the steel sample-slide of the 2π-counter) the geometry of the counting-arrangement was constant, except for differences in the thickness of the samples. All three effects can therefore be considered together as a single self-absorption effect.

Using an identical counting arrangement, and active samples of the same diameter, Cuninghame et al.[56,60] have measured such self-absorption corrections for ten of the nuclides met in this work, and use has been made of their

results. The corrections for the other seven nuclides have been estimated from the available measured data, interpolated to take into account the β-energy of the nuclide concerned.

It should be noted, however, that Cuninghame et al. used different methods in obtaining each of their two groups of self-absorption data. In the first group (ref. 60) the activities of sources of varying weights were compared with that of a weightless source on a 440 $\mu g/cm^2$ Al backing, mounted in the 2π-counter, but with the sample-slide cut away beneath the source. In the second group (ref. 56) the activities of similar thick sources were compared with that of a weightless source on a weightless backing in a 4π-β-proportional counter, similar to that described by Pate and Yaffe.[61]

Only in this second group, therefore, do the correction factors give the absolute activities of the sources directly. However, activities corrected by the data in the first group may be converted to absolute values by comparison of the two sets of data for ^{140}Ba-^{140}La, for which measurements have been made by both methods. (ref. 56, fig. 13 and ref. 60, fig. 9).

Except where a specific reference is given, all the decay-scheme data cited in the ensuing paragraphs have been taken from the compilation by Sullivan.[35]

TABLE III. RESULTS FOR 85m ^{139}Ba

RUN	LENGTH OF IRRADIATION (MINUTES)	CHEMICAL YIELD %	SELF-ABSORPTION FACTOR	SELLOTAPE ABSORPTION FACTOR	PARENT DECAY FACTOR	A^o OBSERVED c.p.m.	A^o CORRECT c.p.m.	S_{139}	MEAN A^o CORRECT
1	20	35.3	0.63	----	--	6.1×10^2	8.00×10^2	---	8.17×10^2
1	20	41.1	0.62	----	--	7.3×10^2	8.35×10^2	---	
2	50	23.3	0.66	0.87	0.8882	3.4×10^3	2.27×10^4	0.1576	2.25×10^4
2	50	40.9	0.65	"	"	5.9×10^3	2.24×10^4	"	
3	60	28.4	0.63	"	"	3.3×10^3	1.86×10^4	0.2937	
4	180	52.4	0.61	"	"	8.7×10^3	2.77×10^4	0.2695	
5	30	85.0	0.59	"	"	3.9×10^4	8.00×10^4	0.3252	
6	150	31.6	0.65	"	"	6.1×10^3	3.05×10^4	0.1481	
7	20	42.1	0.65	"	"	2.2×10^3	8.38×10^3	0.2947	
8	210	40.9	0.65	"	"	1.7×10^4	6.56×10^4	0.1325	
9	240	30.4	0.65	"	"	1.4×10^4	7.17×10^4	0.2564	
10	240	46.7	0.64	"	"	1.9×10^4	6.52×10^4		
10	240	63.3	0.63	"	"	2.5×10^4	6.44×10^4	0.2280	
11	30	23.7	0.66	"	"	7.6×10^3	4.99×10^4	0.3720	
12	240	32.5	0.65	"	"	1.5×10^4	7.30×10^4	0.5161	
13	210	47.7	0.64	"	"	2.5×10^4	8.42×10^4	0.1877	
14	200	49.0	0.64	"	"	2.3×10^4	7.55×10^4	0.1335	
15	60	69.7	0.62	"	"	4.8×10^4	1.14×10^5	0.1793	
16	35	55.3	0.63	"	"	3.2×10^4	9.30×10^4	0.1379	
17	60	32.9	0.65	"	"	4.2×10^4	2.02×10^5	0.3167	
18	240	70.2	0.62	"	"	1.2×10^5	2.90×10^5	0.6389	
19	240	57.0	0.63	"	"	7.6×10^4	2.17×10^5	0.7272	

(a) Results for 85m ^{139}Ba

Because of the ease with which barium may be isolated from fission-product mixtures, and because of its high yield and convenient half-life, ^{139}Ba was adopted as the reference nuclide for all the fission-yield measurements. Its activity was therefore determined in each run, except run 20, when the barium sample was accidentally lost.

To allow for the decay of the ^{139}Cs, the barium separation procedure was never started until 90 minutes after the end of the irradiation, but the samples took only about 30 minutes to prepare, and invariably had initial activities of several thousand c.p.m. (See Table III). These samples were counted at about 20 minute intervals for the first 500 minutes, and thereafter less frequently to determine the activity due to the ^{140}Ba-^{140}La. No difficulty was experienced in resolving the decay-curves, and extrapolating them to obtain the activity at the end of the irradiation.

The results for ^{139}Ba are shown in Table III. The absolute activities (A^{o} correct) have been derived from the observed, extrapolated activities (A^{o} observed) by,

(i) dividing by the chemical yield factor (% yield/100)

(ii) dividing by the sellotape absorption factor (see Table I)

(iii) dividing by the self-absorption factor. This was obtained from the data of Cuninghame et al., ref.56; fig. 12.

(iv) multiplying by a correction factor for the parent (9.5m ^{139}Cs) half-life, since this was not negligible

relative to that of its 85m daughter. This factor was derived as follows:

If ^{139}Cs = 1, and ^{139}Ba = 2, then from equation (II) of the preceding section we have

$$N_2(t') = \frac{B.\sigma.Y_1}{\gamma} \cdot \frac{\lambda_1}{\lambda_2 - \lambda_1} \cdot (e^{-\lambda_1 t''} \cdot S_1 - e^{-\lambda_2 t'} \cdot S_2)$$

where t' is the time of the barium isolation. Since t' was long compared with the half-life of the ^{139}Cs, however, the first term was negligible compared with the second, and therefore

$$N_2^o = N_2(t')/e^{-\lambda_2 t'} = \frac{B.\sigma.Y_1}{\gamma} \cdot \frac{\lambda_1}{\lambda_1 - \lambda_2} \cdot S_2$$

Since $$A_2^o = c_2 . \lambda_2 . N_2^o$$

it will be apparent, that, before substitution in equation (I) of the preceding section, A_2^o must be multiplied by the factor

$$\frac{\lambda_1 - \lambda_2}{\lambda_1} = \frac{\tau_2 - \tau_1}{\tau_2} = \frac{85 - 9.5}{85} = 0.8882$$

RUN	CHEMICAL YIELD %	SELF-ABSORPTION FACTOR	SELLOTAPE ABSORPTION FACTOR	DAUGHTER ACTIVITY FACTOR	A^{o} OBSERVED c.p.m.	A^{o} CORRECT c.p.m.	A^{o}_{139Ba}	Sx	S_{139}	YIELD REL. TO ^{139}Ba	MEAN	NORMALISED YIELD
TABLE IV. RESULTS FOR 2.33h ^{83}Br.												
2	64.3a	0.61	0.66	---	8.4×10^{2}	1.62×10^{3}	2.25×10^{4}	.1734	.1576	.108		
3	62.8a	0.61	"	---	8.2×10^{2}	1.62×10^{3}	1.86×10^{4}	.3218	.2937	.131		
5	42.9b	0.58	"	---	7.3×10^{3}	7.90×10^{4}	8.00×10^{5}	.3433	.3252	.154	0.133	0.622
15	64.5a	0.61	"	---	6.2×10^{3}	1.19×10^{4}	1.14×10^{5}	.2039	.1793	.151	±0.009	±0.042
17	42.5	0.62	"	---	2.9×10^{3}	1.67×10^{4}	2.02×10^{5}	.3538	.3167	.122		

(a) 2 aliquots of stock solution for Br separation (b) Two aliquots of Br carrier solution used.

TABLE V. RESULTS FOR 32m ^{84}Br.												
3	62.8a	0.70	0.95	666	7.2×10^{3}	8.61×10^{3}	1.86×10^{4}	.2080	.2937	.246		
5	42.9b	"	"	---	1.2×10^{4}	4.20×10^{4}	8.00×10^{5}	.2630	.3252	.244	0.245	1.145
15	64.5a	"	"	---	4.4×10^{4}	5.13×10^{4}	1.14×10^{5}	.1170	.1793	.260	±0.006	±0.028
17	42.5	"	"	---	2.3×10^{4}	7.96×10^{4}	2.02×10^{5}	.2040	.3167	.230		

(a) and (b) as for Table IV above.

TABLE VI. RESULTS FOR 10.0h ^{93}Y.												
6	27.5c	0.70	0.91	---	9.8×10^{2}	5.59×10^{3}	3.05×10^{4}	.2772	.1481	1.038		
8	22.5d	"	"	---	1.6×10^{3}	1.12×10^{4}	6.56×10^{4}	.3298	.1325	.965		
12	27.2	"	"	---	3.8×10^{3}	2.14×10^{4}	7.30×10^{4}	1.150	.5161	.925	0.968	4.52
13	15.8	"	"	---	2.8×10^{3}	2.78×10^{4}	8.42×10^{4}	.4639	.1877	.945	±0.025	±0.12

(c) 10 ml aliquot for Y separation, 15 mls for Ba separation. (d) 10 ml aliquot for Y separation, 20 mls for Ba separation.

In the first two runs, and in run 10, duplicate barium samples were prepared, as a check on the reliability of the method of separation. In the first case, the two corrected activities were within about 2% of the mean, whilst in the other runs, better than 1% agreement was obtained.

(b) Results for 2.33h ^{83}Br and 32m ^{84}Br

The decay of the bromine samples was followed for about 12 hours, and the decay-curves so obtained were then easily resolved into their 32- and 140-minute components.

The results for ^{83}Br are shown in Table IV. The self-absorption factors were taken from the data of Cuninghame et al. (ref. 56, fig. 2) and the sellotape absorption factor was derived from the same source, assuming that the sellotape cover was equivalent to 10 mg/cm^2 of aluminium[55] (ref. 56, fig. 14 - aluminium absorption curve for ^{83}Br-^{83m}Br). According to Cuninghame et al. the 32 keV conversion electrons from the 114m ^{83m}Br are completely absorbed in 2 mg/cm^2 Al, and so would not have been counted through the sellotape cover.

The results for ^{84}Br are shown in Table V. The self-absorption, and sellotape absorption, factors for this nuclide were both estimated from available measured data, bearing in mind its high β-energy. (4.68 (40%); 3.56 (9%), 2.53 (16%), 1.72 (35%)).

(c) Results for 10.0h ^{93}Y

The decay of the yttrium samples was followed for about 8 days, by which time the decay-curve could be resolved into its 10-hour and longer-lived components. The longer-lived component was probably the 58d ^{91}Y, but its activity was too low for reliable measurement. Some shorter-lived activity was also present in these samples, but was not identified.

The results for ^{93}Y are shown in Table VI. The self-absorption, and sellotape absorption, factors for this nuclide were both estimated from available measured data, bearing in mind its high (3.1 Mev) β-energy.

(d) Results for 170h ^{97}Zr

The decay of the zirconium samples was followed for about 8 days. After an initial increase in activity, due to the growth of the daughter 74m ^{97}Nb, the samples decayed with the 17-hour half-life appropriate to ^{97}Zr. The activity of the 65d ^{95}Zr was far too low to be measured.

The results for ^{97}Zr are shown in Table VII. The correction for the daughter ^{97}Nb activity was calculated from the decay constants, and for this purpose the intermediate 60s ^{97m}Nb was not taken into account, since its half-life is very short relative to ^{97}Zr and ^{97}Nb, and since it decays

RUN	CHEMICAL YIELD %	SELF-ABSORPTION FACTOR	SELLOTAPE ABSORPTION FACTOR	DAUGHTER ACTIVITY FACTOR	A^o OBSERVED c.p.m.	A^o CORRECT c.p.m.	A^o_{139Ba}	S_x	S_{139}	YIELD REL. TO ^{139}Ba	MEAN	NORMALISED YIELD
TABLE VII. RESULTS FOR 17h ^{97}Zr.												
4	13.4a	0.68	0.82	2.08	6.5×10^2	4.27×10^3	2.77×10^4	.4697	.2695	1.05	1.25 ±0.07	5.85 ±0.33
6	23.2a	0.68	"	"	1.7×10^3	6.50×10^3	3.05×10^4	.2902	.1481	1.31		
8	28.5a	0.66	"	"	5.0×10^3	1.56×10^4	6.56×10^4	.3534	.1325	1.07		
9	14.5a	0.71	"	"	3.5×10^3	2.02×10^4	7.17×10^4	.5483	.2564	1.58		
10	41.4b	0.69	"	"	7.7×10^3	1.59×10^4	6.47×10^4	.6029.	.2280	1.11		
12	84.6b	0.63	"	"	1.6×10^4	1.77×10^4	7.30×10^4	1.179	.5161	1.27		
13	57.3b	0.66	"	"	1.4×10^4	2.17×10^4	8.42×10^4	.4964	.1877	1.17		
19	26.6bc	0.73	"	"	6.0×10^3	1.83×10^4	2.17×10^5	1.298	.7272	1.41		
TABLE VIII. RESULTS FOR 67h ^{99}Mo.												
10	26.8	0.52	0.77	----	5.9×10^2	5.52×10^3	6.47×10^4	.6561	.2280	1.40	1.35 ±0.05	6.31 ±0.23
12	21.5	0.52	"	----	4.9×10^2	5.71×10^4	7.30×10^4	1.266	.5161	1.50		
13	30.3	0.49	"	----	7.3×10^3	6.42×10^4	8.42×10^5	.5342	.1877	1.27		
18i	18.7	0.54	"	----	1.3×10^3	1.72×10^4	2.90×10^5	1.452	.6389	1.23		
18ii	8.4	0.62	"	----	7.4×10^2	1.86×10^4	2.90×10^5	1.452	.6389	1.33		
TABLE IX. RESULTS FOR 4.5h ^{105}Ru.												
3	75.5	0.53	0.65	----	8.5×10^2	3.27×10^3	1.86×10^4	.3430	.2937	.478	0.500 ±0.037	2.34 ±0.17
4	61.3d	0.59	"	----	1.3×10^3	5.62×10^3	2.77×10^4	.4148	.2695	.420		
6	62.3e	0.54	"	----	1.2×10^3	5.26×10^4	3.05×10^4	.2423	.1481	.502		
12	37.4	0.58	"	----	3.5×10^3	2.48×10^4	7.30×10^4	.9277	.5161	.601		

(a) $BaZrF_6$ method (b) Cupferrate extraction method (c) 10 ml aliquot for Zr separation, 25 mls for Ba separation

(d) Half usual amount of Ru carrier used. (e) 10 ml aliquot for Ru separation, 15 mlls for Ba separation

by the emission of 0.75 Mev γ-radiation with few (about 1.5%[62]) conversion electrons.

If ^{97}Zr = 1, and ^{97}Nb = 2, then, when they have reached transient equilibrium,

$$\frac{A_1}{A_2} = \frac{\lambda_2 - \lambda_1}{\lambda_2} = \frac{0.5776 - 0.04078}{0.5776} = 0.9294$$

assuming equal detection coefficients for the two nuclides, since their β-energies are very similar. (See Table I). But the observed activity,

$$A = A_1 + A_2 = A_1(1 + 1/0.9294) = 2.076A_1$$

Therefore, $A_1 = A/2.076$.

The sellotape absorption factor for these samples was measured after the ^{97}Zr-^{97m}Nb-^{97}Nb had reached equilibrium, and the self-absorption factors were taken from the data of Cuninghame et al. (ref. 60, fig. 4).

(e) Results for 67h ^{99}Mo

The decay of the molybdenum samples was followed for about 10 days, and no activity, other than that with the expected 67-hour half-life, was observed. Careful measurements were made of the activities of the freshly prepared samples, both with and without a sellotape covering, to see

if any increase in activity could be detected due to conversion electrons from the 6.04h ^{99m}Tc, which is formed in 87% of the ^{99}Mo disintegrations. No such increase was observed, however, and so no allowance was made for conversion electrons in calculating the absolute activities of the samples.

The results for ^{99}Mo are shown in Table VIII. The sellotape absorption factor was measured for this nuclide (see Table I) and the self-absorption factors were taken from the data of Cuninghame et al. (ref. 60, fig. 5).

(f) Results for 4.5h ^{105}Ru

The decay of the ruthenium samples was followed for about 4 days, and the decay-curves so obtained were then resolved to determine the 4.5h ^{105}Ru activity.

The results for this nuclide are shown in Table IX. The self-absorption factors have been taken from the data of Cuninghame et al. (ref. 56, fig. 4) and the sellotape absorption factor has been derived from the same source, assuming that the sellotape cover was equivalent to 10 mg/cm^2 Al.[55] (ref. 56, fig. 16 - aluminium absorption curve for ^{105}Ru-^{105m}Rh). No correction has been made for any 40s ^{105m}Rh conversion electrons, which were assumed to be completely absorbed in the sellotape cover (γ = 0.13 Mev;

RUN	CHEMICAL YIELD %	SELF-ABSORPTION FACTOR	SELLOTAPE ABSORPTION FACTOR	DAUGHTER ACTIVITY FACTOR	A^{o} OBSERVED c.p.m.	A^{o} CORRECT c.p.m.	$A^{o}_{139_{Ba}}$	S_x	S_{139}	YIELD REL. TO 139_{Ba}	MEAN	NORMALISED YIELD
TABLE X. RESULTS FOR 13.6h ^{109}Pd.												
9	66.4	0.60	0.68	---	1.1×10^{3}	4.18×10^{3}	7.17×10^{4}	.5362	.2564	.267	0.267 ±0.041	1.25 ±0.19
10	23.8	0.66	"	---	6.3×10^{2}	5.86×10^{3}	6.47×10^{4}	.5878	.2280	.337		
12	42.5	0.63	"	---	6.0×10^{2}	3.32×10^{3}	7.30×10^{4}	1.150	.5161	.196		
TABLE XI A. RESULTS FOR 23m ^{111}Pd.												
5	27.6a	0.60	0.85	---	1.3×10^{4}	9.23×10^{4}	8.00×10^{3}	.2282	.3252	.177	0.192 ±0.028	0.90 ±0.13
7	44.3a	0.60	0.85	---	1.8×10^{3}	7.96×10^{3}	8.38×10^{3}	.2271	.2947	.133		
TABLE XI B. RESULTS FOR 7.5d ^{111}Ag.												
12	76.7	0.54	0.70	---	1.1×10^{2}	3.80×10^{2}	7.30×10^{4}	1.276	.5161	.267		
13	54.1	0.57	0.70	---	0.8×10^{2}	3.70×10^{2}	8.42×10^{4}	.5463	.1877	.192		
TABLE XII. RESULTS FOR 21h ^{112}Pd.												
9	66.4	0.55	0.66	2.18	1.1×10^{3}	2.02×10^{3}	7.17×10^{4}	.5579	.2564	.192	0.148 ±0.015	0.69 ±0.07
10	23.8	0.63	0.66	2.18	3.6×10^{2}	1.67×10^{3}	6.47×10^{4}	.6185	.2280	.141		
12	42.5	0.58	0.66	2.18	5.7×10^{2}	1.61×10^{3}	7.30×10^{4}	1.202	.5161	0141		
13	69.9	0.54	0---b	2.18	1.5×10^{3}	1.82×10^{3}	8.42×10^{4}	.5056	.1877	.119		

(a) 25 ml aliquot for Pd separation, 10 mls for Ba separation.

(b) No sellotape cover on this sample.

conversion = 75%).

(g) Results for 13.6h ^{109}Pd and 21h ^{112}Pd

The decay of the palladium samples, prepared for the yield measurements on ^{109}Pd and ^{112}Pd, was followed for about 5 days. Initially, the activities of these samples increased, due to the growth in them of the 3.2h ^{112}Ag; maximum activity was reached about 12 hours after the preparation of the samples. Because of the similarity in the half-lives of the two palladium isotopes, the decay-curves, after the ^{112}Pd-^{112}Ag equilibrium had been established, were resolved by the method of Freilung and Bunney.[63]

If ^{112}Pd = 1, and ^{109}Pd = 2, then by plotting $A(t).e^{\lambda_1 t}$ versus $e^{(\lambda_1-\lambda_2)t}$ a straight line is obtained, having A_2^o as slope, and A_1^o as the intercept on the $A(t).e^{\lambda_1 t}$ axis.

The results for ^{109}Pd are shown in Table X. Because of the presence of the ^{112}Pd in the samples, both the sellotape absorption, and the self-absorption, factors had to be estimated. The 87keV conversion electrons from the 39.2s ^{109m}Ag were assumed to be completely absorbed in the sellotape covering the samples.

The results for ^{112}Pd are shown in Table XII. The correction for the daughter ^{112}Ag activity was calculated from the decay constants.

If ^{112}Pd = 1, and ^{112}Ag = 2, then when they have reached transient equilibrium,

$$\frac{A_1}{A_2} = \frac{\lambda_2 - \lambda_1}{\lambda_2} = \frac{0.2166 - 0.0330}{0.2166} = 0.8475$$

But the observed activity,

$$A = A_1 + A_2 = A_1(1 + 1/0.8475) = 2.18A_1$$

Therefore, $A_1 = A/2.18$.

The sellotape absorption factor was estimated from the available measured data, taking into account the β-energies of the nuclides involved, and their relative abundances:

^{112}Pd, β(MeV) = 0.28

^{112}Ag, β(MeV) = 4.1(25%), 3.6(40%), 2.7(20%), 1.0(15%)

The self-absorption factors were estimated from the data of Cuninghame et al. (ref. 60, fig. 13) for ^{144}Ce+^{144}Pr, which has a very similar decay-scheme to that of ^{112}Pd+^{112}Ag.

(h) Results for 23m ^{111}Pd

The decay of palladium samples, prepared for the yield-measurements on the short-lived ^{111}Pd, was followed for 500 minutes. The decay-curves so obtained were then easily resolved to determine the activity due to the short-lived

RUN	CHEMICAL YIELD %	SELF-ABSORPTION FACTOR	SELLOTAPE ABSORPTION FACTOR	DAUGHTER ACTIVITY FACTOR	A^o OBSERVED c.p.m.	A^o CORRECT c.p.m.	A^o_{139Ba}	S_x	S_{139}	YIELD REL. TO ^{139}Ba	MEAN	NORMALISED YIELD
TABLE XIII. RESULTS FOR 5.3h ^{113}Ag.												
4	73.7	0.57	0.85	---	5.7×10^2	1.59×10^3	2.77×10^4	.4289	.2695	.135		
8	69.0	0.58	0"	---	2.6×10^3	7.69×10^3	6.56×10^4	.2850	.1325	.206		
9	62.0	0.58	"	---	2.5×10^3	8.23×10^3	7.17×10^4	.4619	.2564	.238		
10	73.8	0.57	"	---	2.7×10^3	7.46×10^3	6.47×10^4	.4846	.2280	.203		
11	94.8	0.57	"	---	1.8×10^3	3.94×10^3	4.99×10^4	.4060	.3720	.270		
12	76.7	0.57	"	---	2.8×10^3	7.53×10^3	7.30×10^4	.9742	.5161	.205	0.192 ±0.012	0.898 ±0.056
13	54.1	0.58	"	---	1.9×10^3	7.16×10^3	8.42×10^4	.4021	.1877	.149		
14	75.5a	0.55	"	---	2.5×10^3	7.12×10^3	7.55×10^4	.2847	.1335	.165		
16	86.8a	0.54	"	---	1.8×10^3	4.55×10^3	9.30×10^4	.1467	.1379	.172		
17	97.1a	0.53	"	---	4.4×10^3	1.01×10^4	2.02×10^5	.3872	.3167	.154		
19	72.7a	0.55	"	---	6.6×10^3	1.95×10^4	2.17×10^5	1.127	.7272	.217		
20	86.2a	0.54	"	---	9.1×10^3	2.27×10^4	---	.2263	---	---		

(a) Two aliquots of Ag carrier used.

RUN	CHEMICAL YIELD %	SELF-ABSORPTION FACTOR	SELLOTAPE ABSORPTION FACTOR	DAUGHTER ACTIVITY FACTOR	A^o OBSERVED c.p.m.	A^o CORRECT c.p.m.	A^o_{113Ag}	S_x	S_{113}	YIELD REL. TO $\%^{113}Ag$	MEAN	NORMALISED YIELD
TABLE XIV. RESULTS FOR 21m ^{115}Ag. 9 (b)												
11	94.8	0.65	0.90	---	1.7×10^4	3.07×10^4	3.94×10^3	.2663	.4060	.784		
17	97.1	"	"	---	2.4×10^4	4.23×10^4	1.01×10^4	.1548	.3872	.692	(0.727 ±0.029)	0.654 ±0.049
20	86.2	"	"	---	4.1×10^4	8.13×10^4	2.27×10^4	.0758	.2263	.706		

(b) Results are calculated relative to ^{113}Ag, to make use of Run 20, for which no ^{139}Ba figures are available.

RUN	CHEMICAL YIELD %	SELF-ABSORPTION FACTOR	SELLOTAPE ABSORPTION FACTOR	DAUGHTER ACTIVITY FACTOR	A^o OBSERVED c.p.m.	A^o CORRECT c.p.m.	A^o_{139Ba}	S_x	S_{139}	YIELD REL. TO ^{139}Ba	MEAN	NORMALISED YIELD
TABLE XV. RESULTS FOR 4.6h ^{129}Sb.												
13	54.6	0.63	0.70	1.87	7.4×10^3	1.64×10^4	8.42×10^4	.3841	.1877	.308	0.307 ±0.001	1.43 ±0.01
14	37.7	0.63	0.70	1.87	4.5×10^3	1.45×10^4	7.55×10^4	.2723	.1335	.306		

component. The best fit to the experimental points was given by a line corresponding to a 23-minute half-life, and this figure has been used in calculating the yields of ^{111}Pd.

The results for this nuclide are shown in Table XI A. The sellotape absorption, and self-absorption, factors were estimated from the available measured data for ^{113}Ag, since the β-energies of these two nuclides are very similar (about 2.1 MeV).

(i) Results for 7.5d^{111}Ag and 5.3h^{113}Ag

The decay of the silver samples, prepared for the measurements on the ^{113}Ag, was followed for about two days, by which time the decay-curves could be resolved to determine the 5.3h^{113}Ag activity. The measurements on the samples prepared from the longer irradiations were continued for about two weeks, to determine the activity of the 7.5d^{111}Ag, after which time the activity was too low for reliable measurement.

The results for ^{111}Ag are shown in Table XI B. The self-absorption factors were taken from the data of Cuninghame et al. (ref. 60, fig. 7) and the sellotape absorption factor was estimated by interpolation from available measured data. (See Table I).

The results for ^{113}Ag are shown in Table XIII. The

self-absorption factors were taken from the data of Cuninghame et al. (ref. 56, fig. 5) and the sellotape absorption factor was measured for samples in which the ^{111}Ag intensity was negligible (i.e. samples from the shorter irradiations).

(j) Results for 21m^{115}Ag

For the measurements on ^{115}Ag, the silver samples were quickly prepared after short irradiations, and their decay was followed for long enough to enable the decay-curves to be resolved into their 21-minute and 5.3-hour components.

The results for this nuclide are shown in Table XIV. In order to make use of the results of Run 20, in which a mishap occurred to the barium sample, all the ^{115}Ag yields have been calculated relative to that of ^{113}Ag. The self-absorption, and sellotape absorption, factors for this nuclide were both estimated from available measured data, bearing in mind its high (about 3 MeV) β-energy.

(k) Results for 4.6h^{129}Sb

After an initial increase in activity, due to the growth in them of 74m^{129}Te, the antimony samples decayed with essentially the expected 4.6-hour half-life of ^{129}Sb. The decay of the samples was followed for about 2 days, so that the small

contribution from the long-lived activity present (93h ^{127}Sb ?) could be allowed for.

The results for ^{129}Sb are shown in Table XV. The correction for the daughter ^{129}Te, which is formed directly in 64% of the ^{129}Sb disintegrations, was calculated from the decay constants.

If ^{129}Sb = 1, and ^{129}Te = 2, then, when they have reached transient equilibrium,

$$\frac{A_1}{A_2} = \frac{\lambda_2 - \lambda_1}{\lambda_2} \cdot \frac{100}{64} = \frac{(0.9367 - 0.2510)}{64 \times 0.009367} = 1.142$$

assuming equal detection coefficients for the two nuclides, since their β-energies are very similar. (See Table I). But the observed activity,

$$A = A_1 + A_2 = A_1(1 + 1/1.142) = 1.874A_1$$

Therefore, $A_1 = A/1.874$.

No allowance was made for the ^{129m}Te which is formed in 36% of the ^{129}Sb disintegrations, since its half-life (33d) is long relative to ^{129}Sb and ^{129}Te.

The sellotape absorption factor was measured after the ^{129}Sb-^{129}Te had reached equilibrium, and the self-absorption factors were estimated from the available data for ^{97}Zr-^{97}Nb, which have similar β-energies.

RUN	CHEMICAL YIELD %	SELF-ABSORPTION FACTOR	SELLOTAPE ABSORPTION FACTOR	DAUGHTER ACTIVITY FACTOR	A^{o} OBSERVED c.p.m.	A^{o} CORRECT c.p.m.	A^{o}_{139Ba}	S_x	S_{139}	YIELD REL. TO 139_{Ba}	MEAN	NORMALISED YIELD
TABLE XVI. RESULTS FOR 8.05d ^{131}I.												
8	82.9a	0.40	0.63	---	1.4×10^{2}	6.69×10^{2}	6.56×10^{4}	.3878	.1325	0.955		
9	71.4	0.41	"	---	3.0×10^{2}	1.62×10^{3}	7.17×10^{4}	.5920	.2564	1.341		
12	68.6	0.42	"	---	2.6×10^{2}	1.43×10^{3}	7.30×10^{4}	1.277	.5161	1.088	0.986	4.60
13i	21.2	0.48	"	---	1.0×10^{2}	1.57×10^{3}	8.42×10^{4}	.5463	.1877	0.879	±0.090	±0.42
13ii	59.7	0.43	"	---	1.9×10^{2}	1.17×10^{3}	8.42×10^{4}	.5463	.1877	0.656		
14	45.1a	0.45	"	---	1.0×10^{2}	7.80×10^{2}	7.55×10^{4}	.3810	.1335	0.995		
TABLE XVII. RESULTS FOR 12.8d ^{140}Ba.												
8	40.9	0.53	0.62	2.60	3.1×10^{2}	8.85×10^{2}	6.56×10^{4}	.3890	.1325	0.995		
9	30.4	0.55	"	"	2.1×10^{2}	7.78×10^{2}	7.17×10^{4}	.5936	.2564	1.016		
10	63.3	0.51	"	"	5.3×10^{2}	1.02×10^{3}	6.47×10^{4}	.6707	.2280	1.156		
12	32.5	0.55	"	"	2.2×10^{2}	7.62×10^{2}	7.30×10^{4}	1.284	.5161	0.910	1.00	4.67
13	47.7	0.52	"	"	4.4×10^{2}	1.10×10^{3}	8.42×10^{4}	.5463	.1877	0.973	±0.03	±0.14
14	49.0	0.52	"	"	3.8×10^{2}	9.23×10^{2}	7.55×10^{4}	.3820	.1335	0.928		
18	70.2	0.50	"	"	1.8×10^{3}	3.09×10^{3}	2.90×10^{5}	1.476	.6389	1.000		
TABLE XVIII. RESULTS FOR 32h ^{143}Ce.												
9	47.4	0.48	0.79	---	6.6×10^{2}	3.67×10^{3}	7.17×10^{4}	.5714	.2564	0.520		
10	56.7	0.51	"	---	1.8×10^{3}	7.88×10^{3}	6.47×10^{4}	.6379	.2280	0.980	0.697	3.26
12	66.7	0.50	"	---	1.2×10^{3}	4.56×10^{3}	7.30×10^{4}	1.235	.5161	0.590	±0.140	±0.66

(a) 10 ml aliquot for I separation, 20 mls for Ba separation

(l) Results for 8.05d ^{131}I

The decay of the iodine samples was followed for about 3 weeks, after which their activities became too low for reliable measurement. Although the iodine separations were not begun for some 48 hours after the end of the irradiations, some short-lived activity was always found to be present in the freshly prepared samples. This was probably 2.3h ^{132}I, which has a 78h parent, together with some 21h ^{133}I. The decay-curves could always be resolved without difficulty, however.

The results for ^{131}I are shown in Table XVI. The sellotape absorption factor was measured for this nuclide (see Table I) and the self-absorption factors were taken from the data of Cuninghame et al. (ref. 56, fig. 8).

(m) Results for 12.8d ^{140}Ba

The samples used in the measurements on ^{140}Ba were those prepared from the longer irradiations (i.e. more than 3 hours) for the measurements on ^{139}Ba. Their decay was followed for about 3 weeks, after which their activities became too low for reliable measurement.

The results are shown in Table XVII. The sellotape absorption, and daughter activity, factors have already been discussed (Chapter 4, Part 3). The self-absorption

factors were taken from the data of Cuninghame et al. (ref. 56, fig. 13).

(n) Results for 32h ^{143}Ce

The decay of the cerium samples was followed for about 3 weeks. Due to the presence of undetermined longer- and shorter-lived activities in these samples, the decay-curves were not very easily resolved to obtain the 32-hour component, and this probably accounts for the wide spread in the results which have been obtained.

The results are shown in Table XVIII. The sellotape absorption factor was estimated from available measured data, and the self-absorption factors were taken from the data of Cuninghame et al. (ref. 60, fig. 11).

Part 3 Results for the Xenon Isotopes

(a) Calculating the Yield of ^{133}Xe

For the purpose of calculating the fast-neutron fission-yield of ^{133}Xe, the mass-chain concerned can, with negligible error, be regarded as taking the following simplified form:

$$\underline{133}: \longrightarrow \underset{(1)}{63m\ Te} \xrightarrow[\lambda_1]{} \underset{(2)}{20.8h\ I} \xrightarrow[\lambda_2]{} \underset{(3)}{5.27d\ Xe} \xrightarrow[\lambda_3]{} \text{stable Cs}$$

then, assuming the independent yields of ^{133}I and ^{133}Xe to be negligible compared with the yield of ^{133}Te, the number of nuclei of ^{133}Xe present at the time the xenon is isolated will be given by equation (III), i.e.,

$$N_3(t') = \frac{B.\sigma.Y_1}{\lambda}.(C_1.e^{-\lambda_1 t'}.S_1 + C_2.e^{-\lambda_2 t'}.S_2 + C_3.e^{-\lambda_3 t'}.S_3)$$

where the subscripts refer to the elements in the mass-chain as it is written above. Let us say $Y_1 = Y_{133}$, and write the equation in the abbreviated form:

$$N_3(t') = \frac{B.\sigma.Y_{133}}{\lambda} \cdot f_{133}$$

Now the activity of the ^{133}Xe at time t_i', $A_{133}(t_i')$, can be measured by extrapolating the xenon decay-curve, and then,

$$A_{133}(t_i') = cg_{133}.\lambda_{133} \cdot \frac{B.\sigma.Y_{133}}{\lambda} \cdot f_{133}$$

where cg_{133} = efficiency of the gas-counter for ^{133}Xe, which includes a factor relating the cathode-, and total counter-, volumes.

λ_{133} = decay-constant for ^{133}Xe

An analogous expression can be written for the ^{99}Mo isolated from the same sample of irradiated material; this may be written:

$$A^{o}_{99} = c_{99}.\lambda_{99}. \frac{B.\sigma.Y_{99}}{\gamma} . S_{99}$$

where c_{99} = efficiency of the 2π-counter in counting the ^{99}Mo sample

λ_{99} = decay-constant for ^{99}Mo.

Thus, we may write,

$$\frac{Y_{133}}{Y_{99}} = \frac{A_{133}(t_1')}{A^{o}_{99}} \cdot \frac{\lambda_{99}}{\lambda_{133}} \cdot \frac{S_{99}}{f_{133}} \cdot \frac{c_{99}}{cg_{133}}$$

.....equation (IV).

the unknown factors, B, σ, γ , cancelling between the two equations.

(b) Calculating the Yield of ^{135}Xe

Again, for the purpose of calculating the fast-neutron fission-yield of ^{135}Xe, the mass-chain concerned can, with

negligible error, be regarded as taking the following simplified form:

$$\underline{135}: \longrightarrow \underset{(1)}{6.68h\ I} \xrightarrow[\lambda_1]{} \underset{(2)}{9.13h\ Xe} \xrightarrow[\lambda_2]{} (\text{stable})\ Cs$$

So, assuming the independent yield of ^{135}Xe to be negligible compared with the yield of ^{135}I, the number of nuclei of ^{135}Xe present at the time the xenon is isolated will be given by equation (II), i.e.

$$N_2(t_i') = \frac{B.\sigma.Y_1}{\gamma} \cdot \frac{\lambda_1}{\lambda_2 - \lambda_1} \cdot (e^{-\lambda_1 t_i'}.S_1 - e^{-\lambda_2 t_i'}.S_2)$$

where the subscripts refer to the elements in the mass-chain as it is written above.

Using the same notation as in the previous paragraph, we may write this as

$$N_2(t_i') = \frac{B.\sigma.Y_{135}}{\gamma} \cdot f_{135}$$

and then,

$$\frac{Y_{135}}{Y_{99}} = \frac{A_{135}(t_i')}{A^0_{99}} \cdot \frac{\lambda_{99}}{\lambda_{135}} \cdot \frac{\hat{s}_{99}}{f_{135}} \cdot \frac{c_{99}}{cg_{135}} \quad \text{.....equation (V).}$$

where cg_{135} = efficiency of the gas-counter for ^{135}Xe, which includes a factor relating the cathode-, and total counter-, volumes.

(c) Determination of the Ratio: c_{99}/cg_{133}

Unless the ratio c_{99}/cg_{133} is known, together with the other experimental factors on the right-hand side of equation (IV), then the ratio of the two fission yields (Y_{133}/Y_{99}) cannot be determined. On the other hand, if the yields of these two nuclides were to be known, then the equation could be used to evaluate c_{99}/cg_{133}.

Now the yields of ^{99}Mo and ^{133}Xe are, in fact, very well-known for slow-neutron fission (see, for example, Katcoff[10]) and by substituting these yields in a modified form of equation (IV) the unknown ratio can be evaluated.

For the slow-neutron irradiation (see Chapter 5, Part 5c) the neutron-flux was constant, and so the appropriate equations are:

(i) for ^{99}Mo

$$N^{o}_{99} = B.\sigma.Y'_{99}. \frac{1}{\lambda_{99}}.(1 - e^{-\lambda_{99}T}) = B.\sigma.Y'_{99}. \frac{S'_{99}}{\lambda_{99}}$$

where Y'_{99} refers to the slow-neutron yield of ^{99}Mo, and the other symbols have their usual meaning.

Therefore

$$A^{o}_{99} = c_{99}.B.\sigma.Y'_{99}.S'_{99} \qquad \text{.....equation (VI)}$$

(ii) <u>for ^{133}Xe</u>

For the particular irradiation under consideration, both T and t_i' were long relative to the half-life of the 63m ^{133}Te, so the mass-chain can, with negligible loss of accuracy in this case, be regarded as:

$$\longrightarrow \underset{(1)}{20.8h\ I} \xrightarrow[\lambda_1]{} \underset{(2)}{5.27d\ Xe} \xrightarrow[\lambda_2]{} \text{stable Cs}$$

It can then be shown that the activity of the ^{133}Xe, at the time the xenon is isolated, t_i', is

$$A_{133}(t_i') = cg_{133} \cdot B \cdot \sigma \cdot Y'_{133} \cdot f'_{133} \qquad \text{.....equation (VII)}$$

where, f'_{133} =

$$\frac{\lambda_2}{\lambda_2 - \lambda_1} \cdot \left[e^{-\lambda_1 t_i'} \cdot (1 - e^{-\lambda_1 T}) - e^{-\lambda_2 t_i'} \cdot (1 - e^{-\lambda_2 T}) \right]$$

$$+ \left[e^{-\lambda_2 t'} \cdot (1 - e^{-\lambda_2 T}) \right]$$

Now, from equations (VI) and (VII),

$$\frac{c_{99}}{cg_{133}} = \frac{Y'_{133}}{Y'_{99}} \cdot \frac{f'_{133}}{S'_{99}} \cdot \frac{A^o_{99}}{A_{133}(t_i')} \qquad \text{.....equation (VIII)}$$

and so, by substitution of the published values for Y'_{133} and Y'_{99}, together with the experimental factors, in the right-hand side of this equation, the ratio c_{99}/cg_{133} can be evaluated.

TABLE XIX

Data from Runs 21, 22, and 23

RUN NUMBER:	21[1]	22[1]	23[2]
Duration, T hours	4.00	3.50	432.0
^{99}Mo Data			
Chemical yield, %	46.6	62.2	39.0
Self-absn. factor[3]	0.49	0.46	0.52
Sellotape factor[4]	0.77	0.77	---[5]
A^0 observed	3.85×10^3	9.50×10^3	5.50×10^2
A^0 correct	2.18×10^4	4.31×10^4	2.71×10^3
S_{99}	0.7977	1.326	---
S'_{99}	---	---	0.9885
Xenon Data			
t', hours	11.3	12.3	24.0
% recovery	75.1	78.4	57.3
$A_{133}(t')$ observed	1.8×10^3	3.8×10^3	8.8×10^2
" correct	2.40×10^3	4.85×10^3	1.54×10^3
f_{133}	2.597	4.545	---
f'_{133}	---	---	0.8654
$A_{135}(t')$ observed	2.7×10^4	5.4×10^4	---
" correct	3.59×10^4	6.89×10^4	---
f_{135}	0.3407	0.5584	---

NOTES:
[1] Fast-neutron irradiations.
[2] Slow-neutron irradiations
[3] ex. Cuninghame et al. (Ref. 60, fig. 5)
[4] see Table I
[5] No sellotape cover used.

(d) Results

The data from the runs in which measurements were made of the fission-produced xenon are shown in Table XIX.

Two fast-neutron irradiations (Runs 21 and 22) were carried out, and, as the table shows, high activities were obtained of the three nuclides which were investigated. The decay of both the molybdenum and the xenon samples was followed for about two weeks. In the former, no activity was observed other than that of the 67h ^{99}Mo, whilst the decay-curve obtained from the latter was readily resolved into its 9.13h and 5.27d components, and no other activity was found.

By combining equations (IV) and (V), we obtain

$$\frac{Y_{133}}{Y_{135}} = \frac{A_{133}(t')}{A_{135}(t')} \cdot \frac{\lambda_{135}}{\lambda_{133}} \cdot \frac{f_{135}}{f_{133}} \cdot \frac{cg_{135}}{cg_{153}}$$

so that if one assumes that the efficiency of the gas-counter is the same for both ^{133}Xe and ^{135}Xe, then the relative yields of these two nuclides can be determined from the data from these two runs alone. Table XX shows the results: very close agreement was obtained between the two runs.

TABLE XX

Y_{133}/Y_{135} values

Run No:	21	22	Mean
Y_{133}/Y_{135}	1.218	1.202	1.210 ± 0.008

Since the active xenon formed part of the counter-filling gas, the error introduced by assuming that $cg_{133} = cg_{135}$ is probably not very great. However, the β-energy of ^{135}Xe (0.905 MeV) is higher than that of ^{133}Xe (0.345 MeV), and so, other things being equal, more of the ^{135}Xe β-particles than the ^{133}Xe β-particles would have reached the sensitive cathode volume from the "dead-space" at the ends of the counter. This means that cg_{135} may be slightly bigger than cg_{133}, and the value of Y_{133}/Y_{135} given in Table XX may therefore be lower than the true value.

As was stated in chapter 5, some difficulty was experienced, when carrying out slow-neutron irradiations, in obtaining reasonably high fission-product activities. Eventually this was achieved, but only by irradiating for a relatively long period (18 days in Run 23). As a result, however, the long-lived ^{133}Xe activity was high relative to that of the short-lived ^{135}Xe, and a reliable measurement of the latter could not be made. Unfortunately, time did not permit further slow-neutron irradiations to be carried out, and so the c_{99}/cg_{135} ratio has not been determined.

On substituting the experimental data from Run 23, together with the published values for the slow-neutron (^{235}U) fission-yields of ^{99}Mo and ^{133}Xe, in equation (VIII), the following result is obtained:

$$c_{99}/c_{133} = 1.68$$

where $Y'_{99} = 6.06$; $Y'_{133} = 6.62$; (Katcoff[10]).

This value may then be substituted in equations (IV) and (V), assuming that $cg_{133} = cg_{135}$, with the results shown in Table XXI.

The factors f_{133}, and f_{135}, have been calculated on the assumption that the independent yields of the two xenon nuclides are negligible relative to the total chain yields: in fact this may not be so. A rough calculation shows that, if the independent yield of ^{135}Xe is 0.2% (as it is in slow-neutron fission), the factor f_{135} for Run 21 should be replaced by a factor some 3% bigger. Without a knowledge of the actual independent yields for fast-neutron fission, however, no accurate allowance can be made for this effect.

TABLE XXI

Results for ^{133}Xe and ^{135}Xe

	^{133}Xe	^{135}Xe
(a)		
Yields relative to ^{99}Mo		
Run 21	1.076	0.884
Run 22	1.046	0.870
Mean	1.061 ± 0.016	0.877 ± 0.004
(b)		
Yields relative to ^{139}Ba		
Mean (*)	1.43 ± 0.05	1.18 ± 0.04
(c)		
Normalised Yields		
(^{139}Ba = 4.67%)	6.68 ± 0.23	5.53 ± 0.19

(*) since Y_{99}/Y_{139} = 1.35 ± 0.05 (Table VIII).

CHAPTER 7

DISCUSSION OF RESULTS

The results of all the fission yield measurements are summarised in Table XXII: the standard deviation given in each case is that of the average of the experimental results.

The values for the absolute ("normalised") yields were obtained by first drawing a graph showing the yields of the various nuclei relative to that of ^{139}Ba. The yields of the complementary fragments ("mirror-image" points) were then added, taking the value of ν , the number of prompt fission-neutrons emitted, as 4 (with Cuninghame[28]), which gave the best fit when a curve was drawn through both the experimental points and their mirror-images. (A value of 3 or 5 would give a much poorer fit, particularly on the steeper portions of the curve which, although they contribute relatively little to the total yield, are very sensitive to this value).

The value of ν so deduced, being essentially determined by the yields in the regions where they are a steep function of mass number, can only be identified with $\bar{\nu}$, the average number of prompt neutrons emitted per fission, if one assumes that ν is essentially the same for all modes of fission.

The curve was then normalised in such a manner as to

make the total yield 100% each for the light, and the heavy, fission-product groups. The absolute yields were thereby obtained, and the resulting mass-yield curve is shown in Fig. IX.

For the sake of comparison, the mass-yield curve is shown again in Fig. X, together with those drawn from the results of Cuninghame for ^{238}U-14 MeV neutron fission, and of Richter and Coryell[15] for ^{238}U-16 MeV photofission.

The position of the heavy peak is substantially the same in all three curves, but the light peak from the present results corresponds rather better with the photofission curve than with Cuninghame's 14-MeV curve. Comparison with the photofission curve is valid, since here (with Coryell) 3 prompt neutrons have been assumed per fission. This assumption is justified because of the lower energy of the fissioning ^{238}U nucleus in this case.

The peak-to-trough ratio is 8.8(3) for the light peak, and 9.2(9) for the heavy peak: the mean value, 9.1, agrees with that of Cuninghame, in spite of the difference in the shape of the curves. In the photofission case, where the maximum photon energy was 16-MeV but the effective photon energies were principally 9-14 MeV, this ratio is much larger. This would be expected, because the binding energy of an extra neutron is not here available to add to the excitation energy of the fissioning nucleus.

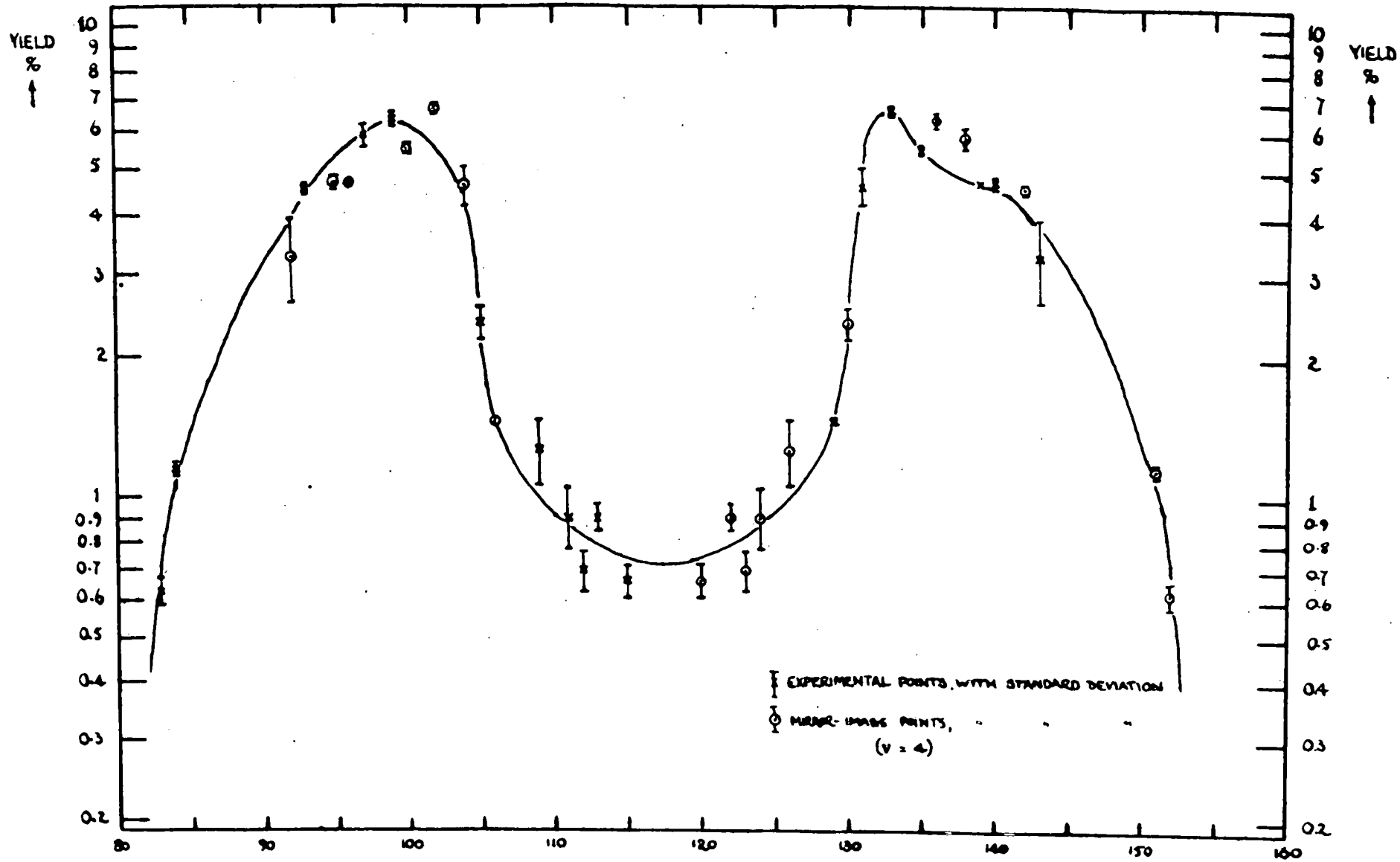

FIG. IX. MASS-YIELD CURVE FOR FISSION OF NATURAL URANIUM BY 14-MEV NEUTRONS.

TABLE XXII

Summary of Results

Mass-number	Nuclide measured	Yield relative to ^{139}Ba	Normalized Yield
83	Br	0.133 ± 0.009	0.62 ± 0.04
84	Br	0.245 ± 0.006	1.15 ± 0.03
93	Y	0.968 ± 0.025	4.52 ± 0.12
97	Zr	1.25 ± 0.07	5.85 ± 0.33
99	Mo	1.35 ± 0.05	6.31 ± 0.23
105	Ru	0.500 ± 0.037	2.34 ± 0.17
109	Pd	0.267 ± 0.041	1.25 ± 0.19
111	Pd/Ag	0.192 ± 0.028	0.90 ± 0.13
112	Pd	0.148 ± 0.015	0.69 ± 0.07
113	Ag	0.192 ± 0.012	0.90 ± 0.06
115	Ag	0.140 ± 0.012	0.65 ± 0.05
129	Sb	0.307 ± 0.001	1.43 ± 0.01
131	I	0.986 ± 0.090	4.60 ± 0.42
133	Xe	1.43 ± 0.05	6.68 ± 0.23
135	Xe	1.18 ± 0.04	5.53 ± 0.19
139	Ba	1.000	4.67
140	Ba	1.00 ± 0.03	4.67 ± 0.14
143	Ce	0.697 ± 0.140	3.26 ± 0.66

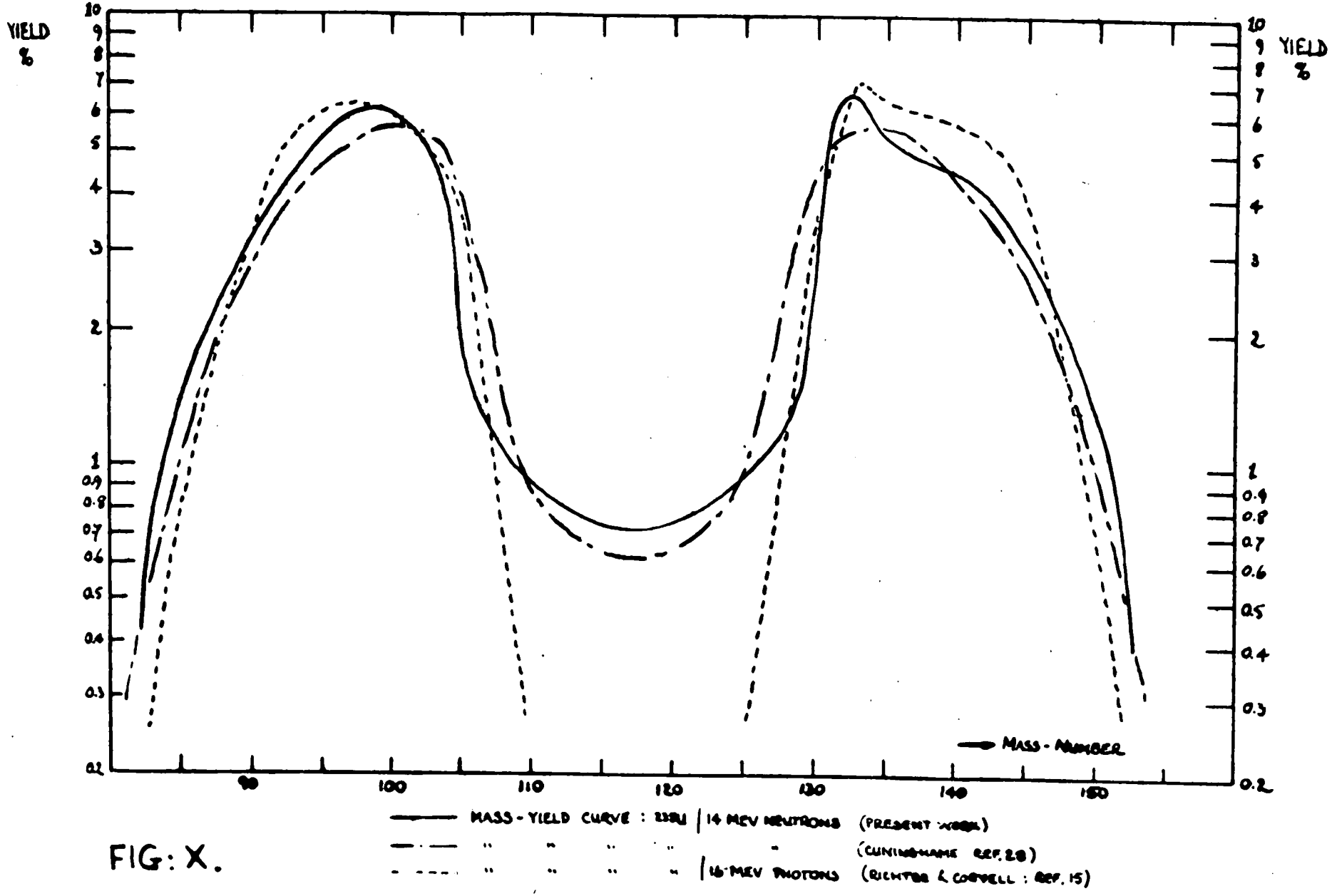
YIELD %
10
9
8
7
6
5
4
3
2
1
0.9
0.8
0.7
0.6
0.5
0.4
0.3
0.2
90
100
110
120
130
140
150
MASS - NUMBER
MASS - YIELD CURVE : 233U | 14 MEV NEUTRONS (PRESENT WORK)
" " " " | " (CUNNINGHAME REF. 28)
" " " " | 16 MEV PHOTONS (RICHTER & CORDELL : REF. 15)

FIG: X.

It is unfortunate that the absolute values which have been obtained for the yields of ^{133}Xe and ^{135}Xe depend upon a single measurement of the ^{133}Xe counting efficiency (made by comparing ^{135}Xe and ^{99}Mo activities from a slow-neutron bombardment). There can be little doubt, however, about the relative yields of the two xenon isotopes (Table XX) and these in themselves seem strongly to indicate the presence of fine structure in the heavy peak, corresponding quite closely with that found in the case of photofission.

Fine structure in this region is generally attributed to the preferential formation of nuclei with a closed shell of 82 neutrons, and if this preference is shown at the actual instant of fission then (as was suggested by Wiles[64] for the case of thermal-neutron fission) it should be reflected in the complementary region around mass 102. Such a reflection has been observed in fine structure in the ^{235}U-thermal neutron mass-yield curve.[10]

Since no experimental points fall in the region between mass 99 and 105, it cannot definitely be stated that such fine structure is absent from the light peak in the present case. For the purpose of normalisation, however, a smooth curve through the available experimental points gives the best result, and this suggests that the observed fine structure is due to the emission of delayed neutrons from certain of the heavy fragments, after the actual fission event has taken place.

This would add weight to the argument that, in high-energy fission, there is a lessening of the influence of the 82-neutron shell on the actual mode of fission which occurs, and that this, in itself, is responsible for the increasing favour for symmetrical modes of fission which is observed in such cases.

It should be pointed out, however, that, as a result of a close investigation of the yields in the region of masses 131-135, Wahl[27] has concluded that there is little or no evidence for fine structure in this part of the mass-yield curve for fission of ^{235}U by 14-MeV neutrons. He has found, on the other hand, that the independent yields of the later members of the chains in this region are considerably higher than they are for thermal neutron fission, indicating a shift towards stability of the most probable initial nuclear charge.

The results reported in this thesis, then, are sufficient to show that the mass-yield curve for fission of ^{238}U by 14-MeV neutrons does fit in with the general pattern of such curves. Further, in parallel with the findings for photofission, there is evidence that the 82-neutron shell continues to exert a perturbing influence on the fission yields.

In the light of Wahl's paper, however, it is clearly desirable that a more intensive investigation should be made

of the yields in the regions where fine structure might be expected to occur: i.e. in the regions, not only of the 82-neutron shell, and of its complementary fragments, but also of the 50-neutron, and 50-proton, shells. (In the latter regions, however, fine structure effects may be very much obscured by the rapid changes in yield with mass-number which occur).

The measurement, wherever possible, of the independent yields of nuclei is particularly to be desired, so that a picture of the distribution of nuclear charge in this form of fission may be built up. It seems likely that in this distribution may lie one of the essential differences between high, and low, energy fission, and a better understanding of this difference would be a valuable step towards a better understanding of the fission process as a whole.

REFERENCES

1. Hahn O., and Strassmann F.: Naturwiss., 27, 11, (1939)
2. Inghram M.C.: Annual Reviews of Nuclear Science, 4, 81, (1954)
3. Petruska J.A., Thode H.G. and Tomlinson R.H.: Can. J. Phys., 33, 693, (1955)
4. Steinberg E.P. and Glendenin L.E.: International Conf. on the Peaceful Uses of Atomic Energy: Proceedings, vol. 7, paper 614 (United Nations, New York, 1956)
5. Baerg A.P. and Bartholomew R.M.: Can. J. Chem., 35, 980, (1957)
6. see, for example: Rossi B.B. and Staub H.H.: "Ionisation Chambers and Counters" National Nuclear Energy Series, Div. V, vol. 2, chapter 9 (McGraw-Hill, New York, 1949)
7. see, for example: Chapter 8 of ref. 6.
8. de Laboulaye H., Tzara C. and Olkowsky J.:
   (i) Compt. rend., 237, 155, (1953)
   (ii) J. de phys. radium, 15, 470, (1954)
9. Whitehouse W.J.: Progress in Nuclear Physics, 2, 120, (1952)
10. Katcoff S.: Nucleonics, 16, No. 4, 79, (April 1958)
11. Goeckermann R.H. and Perlman I.: Phys. Rev., 76, 628, (1949)

12. MacNamara J. and Thode H.G.: Phys. Rev., 80, 471, (1950)

13. Purkayastha B.C. and Martin G.R.: Can. J. Chem., 34, 293, (1956)

14. Kuroda P.K. and Edwards R.R.: J. Inorg. and Nuc. Chem., 3, 345, (1957)

15. Richter H.G. and Coryell C.D.: Phys. Rev., 95, 1550, (1954)

16. Folger R.L., Stevenson P.C. and Seaborg G.T.: Phys. Rev., 98, 107, (1955)

17. Hicks H.G., Stevenson P.C., Gilbert R.S. and Hutchin W.H.: Phys. Rev., 100, 1284, (1955)

18. Hicks H.G. and Gilbert R.S.: Phys. Rev., 100, 1286, (1955)

19. Sugihara T.T., Drevinsky P.J., Troianello E.J. and Alexander J.M.: Phys. Rev., 108, 1264, (1957)

20. Lavrukhina A.K. and Krasavina L.D.: J. Nuc. Energy (II) 5, 236, (1957)

21. Hollander J.M.: U.C.R.L.-1396, (1951)

22. Brown F., Price M.R. and Willis H.H.: J. Inorg. and Nuc. Chem., 3, 9 (1956)

23. Ghiorso A., Rossi G.B., Harvey B.G. and Thompson S.G.: Phys. Rev., 93, 257, (1954)

24. Lamphere R.W.: Phys. Rev., 104, 1654, (1956)

25. Spence R.W.: U.S.A.E.C. Report A.E.C.D. 2625 (1949)

26. Terrell J., Scott W.E., Gilmore J.S. and Minkinnen C.O.: Phys. Rev., 92, 1091, (1953)

27. Wahl A.C.: Phys. Rev.: 99, 730, (1955)

28. Cuninghame J.G.: J. Inorg. and Nuc. Chem., 5, 1, (1957)

29. Glendenin L.E. and Steinberg E.P.: Annual Reviews of Nuclear Science, 4, 69, (1954)

30. Spence R.W. and Ford G.P.: Annual Reviews of Nuclear Science, 2, 399, (1953)

31. Coryell C.D. and Sugarman N. (Eds): "Radiochemical Studies: The Fission Products". National Nuclear Energy Series, Div. IV, vol. 9. (McGraw-Hill, New York, 1951)

32. Hanson A.O., Taschek R.F. and Williams J.H.: Rev. Mod. Phys. 21, 635, (1949)

33. Martin E.B.M.: unpublished handbook, Londonderry Laboratory for Radiochemistry, University of Durham.

34. Graves E.R., Rodrigues A.A., Goldblatt M. and Meyer D.I.: Rev. Sci. Inst., 20, 579, (1949)

35. Sullivan W.H.: "Trilinear Chart of Nuclides" (U.S.A.E.C. January 1957)

36. Glendenin L.E.: Paper 288, p. 1657, of ref. 31.

37. Glendenin L.E., Edwards R.R. and Gest H.: Paper 232, p. 1451, of ref. 31.

38. Glendenin L.E. and Metcalf R.P.: Paper 278, p. 1625, of ref. 31.

39. Ballou N.E.: Paper 292, p. 1673, of ref. 31.

40. McKay H.A.C. and Fletcher J.M.: Progress in Nuclear Energy, Series III, vol. 1, p. 147 (Pergamon Press, London, 1956)

41. Warf J.C.: J.A.C.S., 71, 3257, (1949)

42. Scargill D., Alcock K., Fletcher J.M., Hesford E. and McKay, H.A.C.: J. Inorg. and Nuc. Chem., 4, 304, (1957)

43. Hume D.N.: Paper 245, p. 1499, of ref. 31.

44. Furman N.H., Mason W.B. and Pekola J.S.: Anal. Chem., 21, 1325, (1949)

45. Oesper R.E. and Klingenberg J.J.: Anal. Chem., 21, 1509, (1949)

46. Kumins C.A.: Anal. Chem., 19, 376 (1947)

47. Hahn R.B.: Anal. Chem., 21, 1579, (1949)

48. Ballou N.E.: Paper 257, p. 1538, of ref. 31.

49. Vogel A.I.: "Quantitative Inorganic Analysis", p. 523 (Longmans, Green and Co., London, 1948)

50. White C.E. and Rose H.J.: Anal. Chem., 25, 351, (1953)

51. Boldridge W.F. and Hume D.N.: Paper 272, p. 1595, of ref. 31.

52. Glendenin L.E.: Paper 260, p. 1549, of ref. 31.

53. Glendenin L.E.: Paper 265, p. 1575, of ref. 31.

54. Glendenin L.E.: Paper 267, p. 1580, of ref. 31.

55. James R.H.: Private communication.

56. Cuninghame J.G., Sizeland M.L. and Willis H.H.: A.E.R.E. C/R 2054 (1957)

57. Epstein S.: Proceedings of the Conf. on Nuclear Chem., p. 108, (McMaster University, Hamilton, Ontario, 1947)

58. Arrol W.J., Chackett K.F. and Epstein S.: Can. J. Research, 27B, 757, (1949)

59. Wilkinson, D.H.: "Ionisation Chambers and Counters", p. 45, (Cambridge Univ. Press, 1950)

60. Cuninghame J.G., Sizeland M.L. and Willis H.H.: A.E.R.E. C/R 1646 (1955)

61. Pate B.D. and Yaffe L.: Can. J. Chem., 33, 610, (1955)

62. Burgus W.H., Knight J.D. and Prestwood R.J.: Phys. Rev., 79, 104, (1950)

63. Freilung E.C. and Bunney L.R.: Nucleonics, 13, No. 9, 112, (Sept. 1956)

64. Wiles D.R.: M.Sc. Thesis (McMaster University, Hamilton, Ontario, 1950), quoted by Steinberg and Glendenin, ref. 4.

ACKNOWLEDGEMENTS

I wish to record my most sincere thanks to the following:

Mr. G.R. Martin, Reader in Radiochemistry in the University of Durham, under whose supervision this work was carried out, for his keen interest and sound advice, and for the benefit, in many discussions, of his wide knowledge of all aspects of radiochemistry.

Mr. R.H. James, in collaboration with whom much of the early experimental work was undertaken, for his permission to make use of many of his results in this thesis, and for his cheerful help and companionship.

Mrs. E.B.M. Martin, for her kind assistance in running the neutron-generator on several occasions.

The Council of the Durham Colleges for the award of a Research Studentship, during the tenure of which this work was undertaken.

D.J. Silvester.